

USAARL REPORT NO. 76-13
VOLUME I

COMPUTER MODELING OF THE BODY-HEAD-HELMET SYSTEM

By

Wartan A. Jemian
Nan-Heng Lin

School of Engineering, Auburn University
Auburn, Alabama 36830

February 1976

Final Report

This document has been approved for public release and sale; its
distribution is unlimited.

Prepared for:

Bioengineering and Evaluation Division
US Army Aeromedical Research Laboratory
Fort Rucker, Alabama 36362



NOTICE

Qualified requesters may obtain copies from the Defense Documentation Center (DDC), Cameron Station, Alexandria, Virginia. Orders will be expedited if placed through the librarian or other person designated to request documents from DDC (Formerly ASTIA).

Change of Address

Organization receiving reports from the US Army Aeromedical Research Laboratory on automatic mailing lists should confirm correct address when corresponding about laboratory reports.

Disposition

Destroy this report when it is no longer needed. Do not return it to the originator.

Disclaimer

The findings in this report are not to be construed as an official Department of the Army position unless so designated by other authorized documents.

REPORT DOCUMENTATION PAGE		READ INSTRUCTIONS BEFORE COMPLETING FORM
1. REPORT NUMBER	2. GOVT ACCESSION NO.	3. RECIPIENT'S CATALOG NUMBER
4. TITLE (and Subtitle) Computer Modeling of the Body-Head-Helmet System Volume I		5. TYPE OF REPORT & PERIOD COVERED Report for publication
7. AUTHOR(s) Wartan A. Jemian Nan-Heng Lin		6. PERFORMING ORG. REPORT NUMBER
9. PERFORMING ORGANIZATION NAME AND ADDRESS Auburn University School of Engineering Auburn, AL 36830		8. CONTRACT OR GRANT NUMBER(s) DABT01-74-C-0231
11. CONTROLLING OFFICE NAME AND ADDRESS Bioengineering and Evaluation Division US Army Aeromedical Research Laboratory Fort Rucker, AL 36362		10. PROGRAM ELEMENT, PROJECT, TASK AREA & WORK UNIT NUMBERS DD Form 1498
14. MONITORING AGENCY NAME & ADDRESS (if different from Controlling Office) USA Medical Research and Development Command Washington, DC 20314		12. REPORT DATE December 1975
		13. NUMBER OF PAGES 83
		15. SECURITY CLASS. (of this report) Unclassified
		15a. DECLASSIFICATION/DOWNGRADING SCHEDULE
16. DISTRIBUTION STATEMENT (of this Report) This document has been approved for public release and sale; its distribution is unlimited.		
17. DISTRIBUTION STATEMENT (of the abstract entered in Block 20, if different from Report)		
18. SUPPLEMENTARY NOTES		
19. KEY WORDS (Continue on reverse side if necessary and identify by block number) Crash Helmet Computer Simulation Finite Element Structural Analysis Inertial Properties Severity Index Stress Field Displacement Acceleration Profile Three Dimensional Finite Element		
20. ABSTRACT (Continue on reverse side if necessary and identify by block number) Three dimensional finite element methods of analysis were applied to the body-head-helmet structural system under conditions of static equilibrium and to the head-helmet assembly in a dynamic mode. Computer programs were written to generate the three dimensional grids, to evaluate inertial properties, and to process and display results of the structural analyses. Structural analyses were performed using Structural Analysis Program IV supplied by the University of California.		

Unclassified

SECURITY CLASSIFICATION OF THIS PAGE(When Data Entered)

Static analysis, using a fixed configuration, is applicable to the description of displacement and stress component fields in the system. The results of this mode of analysis have the potential of yielding information related to loss of consciousness due to impact situations.

Dynamic structural analysis was performed on a computer generated pseudospherical model simulating the drop test. Results provide time traces of the displacement, velocity, acceleration, and stress components at selected nodal points and elements of the system.

Methods were demonstrated for the determination of a number of parameters of potential or proven value in evaluating crash protection or crash severity. These include linear acceleration profile, rotational acceleration profile, shear stress, skull deflection, severity index, mass moments of inertia, and regional centers of gravity. Six specific recommendations were made for steps to be taken in applying finite element simulation to helmet design. These include the development of a head form simulation in the dynamic mode and the addition of elements to represent nonlinear and anisotropic materials behavior to portions of the system as appropriate.

Unclassified

SECURITY CLASSIFICATION OF THIS PAGE(When Data Entered)

SUMMARY

Three dimensional finite element methods of analysis were applied to the body-head-helmet structural system under conditions of static equilibrium and to the head-helmet assembly in a dynamic mode. Computer programs were written to generate the three dimensional grids, to evaluate inertial properties, and to process and display results of the structural analyses. Structural analyses were performed using Structural Analysis Program IV supplied by the University of California.

Static analysis, using a fixed configuration, is applicable to the description of displacement and stress component fields in the system. The results of this mode of analysis have the potential of yielding information related to loss of consciousness due to impact situations.

Dynamic structural analysis was performed on a computer generated pseudospherical model simulating the drop test. Results provide time traces of the displacement, velocity, acceleration, and stress components at selected nodal points and elements of the system.

Methods were demonstrated for the determination of a number of parameters of potential or proven value in evaluating crash protection or crash severity. These include linear acceleration profile, rotational acceleration profile, shear stress, skull deflection, severity index, mass moments of inertia, and regional centers of gravity. Specific recommendations were made for applying finite element simulation to helmet design.

Approved:


ROBERT W. BAILEY
Colonel, MSC
Commander

TABLE OF CONTENTS
VOLUME 1

SUMMARY.	
I. INTRODUCTION	1
A. Objective	1
B. Human Tolerance	2
C. Helmet Design	3
D. Testing	4
E. Simulation	5
II. FINITE ELEMENT SIMULATION.	9
A. The Structural System	9
B. Stereographic Drawings	16
C. Inertial Properties.	16
1. Nodal Points	16
2. Elements	17
3. Centers of Gravity.	17
4. Element Volume.	20
5. Element Mass	21
6. Mass Moment of Inertia.	21
7. Element Group Properties.	21
D. Static Structural Analysis	22
1. Variables and Equations	23
2. Solution and Results.	24
3. Accuracy and Execution Time	25
E. Dynamic Structural Analysis	25
F. General Comments on Computer Operation	27
III. RESULTS: STATIC ANALYSIS.	30
A. System Mechanics	30
1. Linear Deformation	30
2. Relationship to Dynamic Loading	30

B.	System Formation and Characteristics	31
1.	Dimensions	31
2.	Mass.	33
3.	Inertial Moments	36
4.	Stress Field	39
C.	Effect of Inner Liner Modulus	40
1.	Materials Properties	40
2.	Displacements	43
3.	Skull Deflection	46
4.	Stresses	46
5.	Work of Deformation	52
IV.	RESULTS: DYNAMIC ANALYSIS	55
A.	Drop Test Simulation	56
B.	The Configuration	56
C.	Inertial Properties	57
D.	Boundary Conditions and Inertial Loading	62
1.	Loading Points	62
2.	Ground Acceleration	62
3.	Displacement Time Trace	64
4.	Rotational Acceleration	66
E.	Effect of Inner Liner Modulus Variation	70
1.	Aluminum Head Form	70
2.	Humanoid Head Form	72
3.	Severity Index	72
V.	SUMMARY AND RECOMMENDATIONS FOR FURTHER WORK	76
A.	Inertial Properties Analysis	76
B.	Structural Analysis	77
C.	Injury Parameters	78
D.	Recommendations for Further Research	78
VI.	CONCLUSIONS	82
	BIBLIOGRAPHY	84

TABLE OF CONTENTS
VOLUME II

Section I -	The Fixed Body-Head-Helmet Configuration	86
	Identity of 382 Nodal Point Coordinates and Boundary Conditions	
Section II -	The 3X3X3 Pseudosphere Head-Helmet Model,	105
	Identity of 87 Nodal Point Coordinates and Boundary Conditions	
Section III -	Computer Service Listing in FORTRAN, The	112
	Facilities and Subprograms of the IBM Operating System and Calcomp Plotter	

I. INTRODUCTION

A. Objective

The objective of this engineering research was to write computer programs to aid in the design of crash protection helmets for army airmen. Computer simulation represents a new design procedure in this field although it has been used in other fields and is gaining in acceptance. The digital computer has the storage capacity and speed that make it possible for as complex a system as the human torso, head, and a crash helmet to be contained in considerable detail and manipulated mathematically as a single abstract structural entity.

It is necessary to include major portions of the body with the helmet in order to better simulate crash circumstances. This inclusion affects the direction, magnitude and sequence of impulses. Although this could be extended to include the entire body it was felt that army airmen would probably be belted into seats in the aircraft with relatively little unrestricted motion possible, and therefore the torso should provide the necessary information.

Originally it was planned to model the body, head, and helmet in a two dimensional, static simulation, but early in the course of the research it was found to be possible to extend the representation to three dimensions and in a dynamic mode. The scope of the research was expanded to include the study and demonstration of several possible methods of finite element simulation and the determination of specific parameters of importance to human safety and crash protection.

B. Human Tolerance

The crash protection needs of Army airmen are critically important with respect to head protection. Most fatalities result directly or indirectly through head injury. A crash helmet can provide protection against penetration by sharp objects, distribute a concentrated load which might cause excessive deflection of the skull and concussion, and reduce the deceleration of the skull and brain during crash impact.

Holbourn (10)* reported the effect of shear strain on damage to the brain. His observations were both clinical and experimental using gelatinous models. Many other investigators have continued along the same directions, examining shear as a possible index of human tolerance.

Gurdjian (7) found that continued acceleration is damaging and reported a relation between average acceleration and time of exposure. This is now known as "The Wayne State University Cerebral Concussion Tolerance Curve". Gadd (5) incorporated this and other data to yield a severity index of the form $a^{2.5}t$, where a is the acceleration in gravitational units and t is time in seconds. Conditions corresponding to a Gadd severity index of 1000 or more are critical. These criteria represent the limits of human tolerance although instances have been reported of greater tolerance as well as lesser. An important feature of the Wayne State Curve is that it shows no apparent limit to the time that accelerations below 42g can be tolerated. The bulk of the evidence that is accumulating supports acceleration as an important criterion.

Hardy and Marcal (9) cited skull deflection as a criterion and used two dimensional finite element structural analysis to compute skull

*Numbers in parentheses refer to listings in BIBLIOGRAPHY.

deflections. A similar study was recently reported by Chan (3).

This may have its effect through pressure on the brain, which has not been as actively supported as a mechanism as cavitation in the brain.

Ommaya (13) and others have indicated that head angular acceleration is injurious. Thus there are now a variety of parameters that may be used as measures of severity of impact situations. As information is accumulated in this growing field of investigation other parameters will be found. Each may be computed from the results of the simulation.

C. Helmet Design

Helmet design has progressed under several driving forces. First there is the basic need to afford protection to the head, second there is the desire on the part of the systems engineer to attach peripheral equipment to the helmet to serve various other functions and third there is the limited tolerance of the person wearing the helmet for additional loads on the head. There is no question but that a limit exists to the amount of protection that may be provided by a helmet or any other safety device. The objective in helmet design is to extend the protection to include as many and as severe crash situations as possible. Extending the range of protection then dictates that any peripheral devices be eliminated unless they provide a vital function that cannot be provided in some other manner and that the most efficient design be used to combine materials for the utmost in mechanical protection at a minimum of weight. Parameters such as helmet weight, center of gravity and inertial moments may be easily computed for purposes of

evaluation. The relationship of Gurdjian dictates that the time over which the head is subjected to deceleration be reduced to a minimum in keeping with the exposure-acceleration curve. For this reason the inner liner material used to absorb energy should not only be relatively soft and compressible but should recover shape slowly. This material should deform under the action of the impact to allow the head to be gradually brought to a new state of motion but should not immediately spring back because, if allowed, the period during which the head is subjected to the accelerations will be almost doubled. Present helmet designs incorporate energy absorbing materials with these properties. Other features of helmets in current use are a harness system of straps and deformable clips attached to the inside of the helmet. The harness provides another "no-spring-back" energy absorbing system as well as ventilation between the head and the helmet. The helmet shell provides protection against penetrating objects and distributes concentrated loads.

A recent investigation by Haley et. al. (8) showed the desirability of using a multiple layer helmet design. In this system there are essentially two relatively compliant energy absorbing layers and two relatively thin and stiff structural shells. The outer shell resists penetration and distributes load and the inner shell further distributes load. This design is typical of those that must be considered to extend the range of head protection.

D. Testing

Helmet testing is usually conducted in a drop test in which the helmet is attached to a head form, approximating the shape of a human

head, with the same overall weight and with an accelerometer attached at the center of gravity. The head form is dropped from a predetermined height onto a surface of controlled stiffness. The helmet is dropped with the head form and the amount of acceleration transmitted to the center of gravity of the head form is a measure of the effectiveness of the helmet. This type of testing requires helmet construction and usually results in either partial or total destruction of the helmet. This is a direct means of quality control in helmets that are to be used by airmen but is expensive and time consuming. The principal advantage is, of course, the fact that the actual helmet may be tested under conditions that approximate use and extend into the range of severity of testing that would be beyond any that could be performed with living persons. Direct testing is limited to conditions that are both non-injurious and acceptable to the persons involved. The parameters measured in the drop test may be computed from the results of a simulation.

E. Simulation

Simulation is necessary for safety and economy. In a simulation it is also possible to maintain certain parameters constant and vary others at will. This is desirable to produce specific information. There are essentially three approaches to simulation: experimental simulation involving cadavers, mannikins, head forms, and other physical devices; mathematical simulation in which the system is represented by a series of physical parameters in the form of a simplified model, the response of the model to certain external actions is expressed as a

single or set of differential equations to be solved in closed form or computationally (finite difference methods etc.); and computational simulation, generally employing matrix analytical methods to be carried out by high speed, high storage capacity digital computers. Each of these simulation methods offers advantages and disadvantages. Experimental simulation is relatively direct but suffers from all of the usual human errors and complexities of instrumentation involved with fabrication, testing, and interpretation. Mathematical simulation, which is most promising with respect to the general value of the equations that result from the analysis, is subject to severe limitations in terms of the difficulty of solving any but the most simple equations.

The approach taken in this research is to simulate using a three dimensional finite element computational procedure. The advantage is that the constitutive equations may be applied to simple, three dimensional volume elements which are homogeneous in all respects and are assigned properties to represent selected regions of the system. The reactions of each element to action from neighboring elements and ultimately from surface actions are expressed in a direct set of equations. The total set of equations for the entire system is then solved simultaneously using the capabilities of the digital computer.

The heart of the simulation is in the selection of the three dimensional elements; and this, of course, leads to any approximation or error in the results of the analysis. The degree of approximation is, however, subject to analysis and any error may be reduced to a tolerable and practical extent by redefining element sizes and shapes. A complete

finite element structural analysis should include this consideration and usually involves a number of separate determinations with different configurations of finite element grids.

Simulation or modeling systems should provide for representations of:

1. Overall structure shape
2. Mass distribution
3. Kinematics of the components within the system
4. Mechanics of the various materials employed
5. The mechanics of the system as a unit.

A computer modeling system should provide for:

1. Generation of coordinates
2. Calibration of the system to ensure proper shape, mass distribution, kinematics, etc.
3. Analytical capabilities to determine centers-of-gravity, inertial moments, etc.
4. Features to facilitate comparisons
5. Methods for convenient output of data such as three dimensional projective drawings.

In this research a number of computer programs were written to provide the above features in essentially two methods of simulation, fixed nodal points or parametric, which is computer generated. Both three-dimensional finite element inertial property analyses, and two modes of structural analyses were performed. One mode is a static representation based on a balance of forces which must be compared, indirectly, to the dynamic situations that occur. The second is a dynamic analysis which

provides time traces. These two methods are demonstrated and explained in the third and fourth sections of this report. The next section presents a brief review of finite element methods of analysis. Appendix A is a listing of the nodal point coordinates and connection arrays for the static model, Appendix B is a similar listing for the dynamic model, and Appendix C is a listing of SERVICE which performs all of the special functions except structural analysis.

II. FINITE ELEMENT SIMULATION

A. The Structural System

The human body is a complex composite structural system supported by approximately 206 bones and operated by approximately 300 pairs of muscles. The materials of the other parts of the system contribute mass and shape but are not active structural elements. The bones are in contact at the joints in a manner that allows them to pivot relatively freely. Each motion in the body is produced by opposing actions, contraction and relaxation, in the muscle groups.

Bone is a composite material with characteristic materials properties listed in Table 1; and muscle is a composite viscoelastic material, also with characteristic properties. A unique characteristic of the muscle is that it is capable of producing mechanical action. Other characteristic properties of the materials in the human body are listed in Table 1. Table 2 is a compilation of appropriate anthropometric data.

The principal structural member in the upper portion of the body is the spinal column which consists of seven cervical, twelve thoracic and five lumbar vertebrae counted from the head down. The general shape of the spinal column is shown in Figure 1. Each vertebra is effectively a stiff structural member that is in contact with the neighboring vertebrae through thin, relatively frictionless layers. A three dimensional finite element representation of the spinal column is shown in Figure 2 as a column of seven "brick type" volume elements. These elements can be assigned properties from Table 1 as a first approximation but structural analysis shows that the spinal column determined in this way is too

TABLE 1
 PROPERTIES OF MATERIALS IN THE HUMAN BODY

Property, Dimensions	Bone	Materials Flesh	Brain
Density, g cm ⁻³	1.94	1.00	1.05
Youngs Modulus, MPa	1.1 x 10 ⁵	-	-
Bulk Modulus, MPa	1.6 x 10 ⁴	-	2.1 x 10 ³

TABLE 2
ANTHROPOMETRIC DATA

Segment Description	(1)*	Measurement	(4)*
Lengths, cm			
Head Breadth	15.49		14.3
Head Length	19.56		18.9
Head Height	23.62		25.0
Sitting Height	79.25		97.9
Chest Breadth	25.00		33.4
Chest Depth	22.86		22.6
Neck Breadth	6.20		-
Weights, kg			
Head	5.08		4.76
Torso	18.28		17.86
Torso and Head	23.36		22.62

* Measurements are from references (1) and (4) in the BIBLIOGRAPHY.

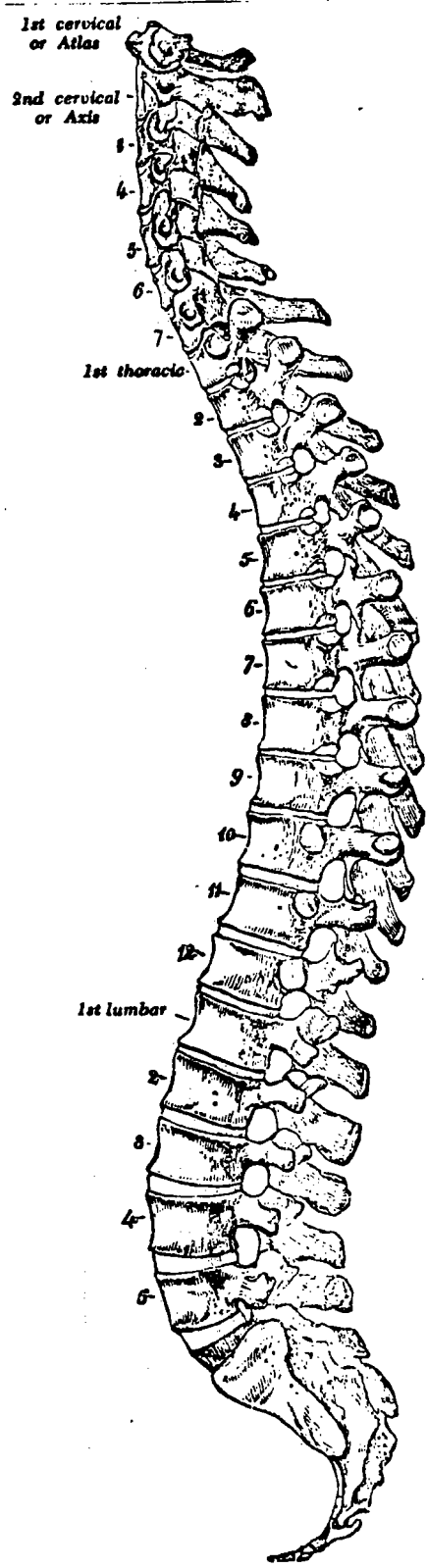


Figure 1. Lateral view of the vertebral column (6, page 301).

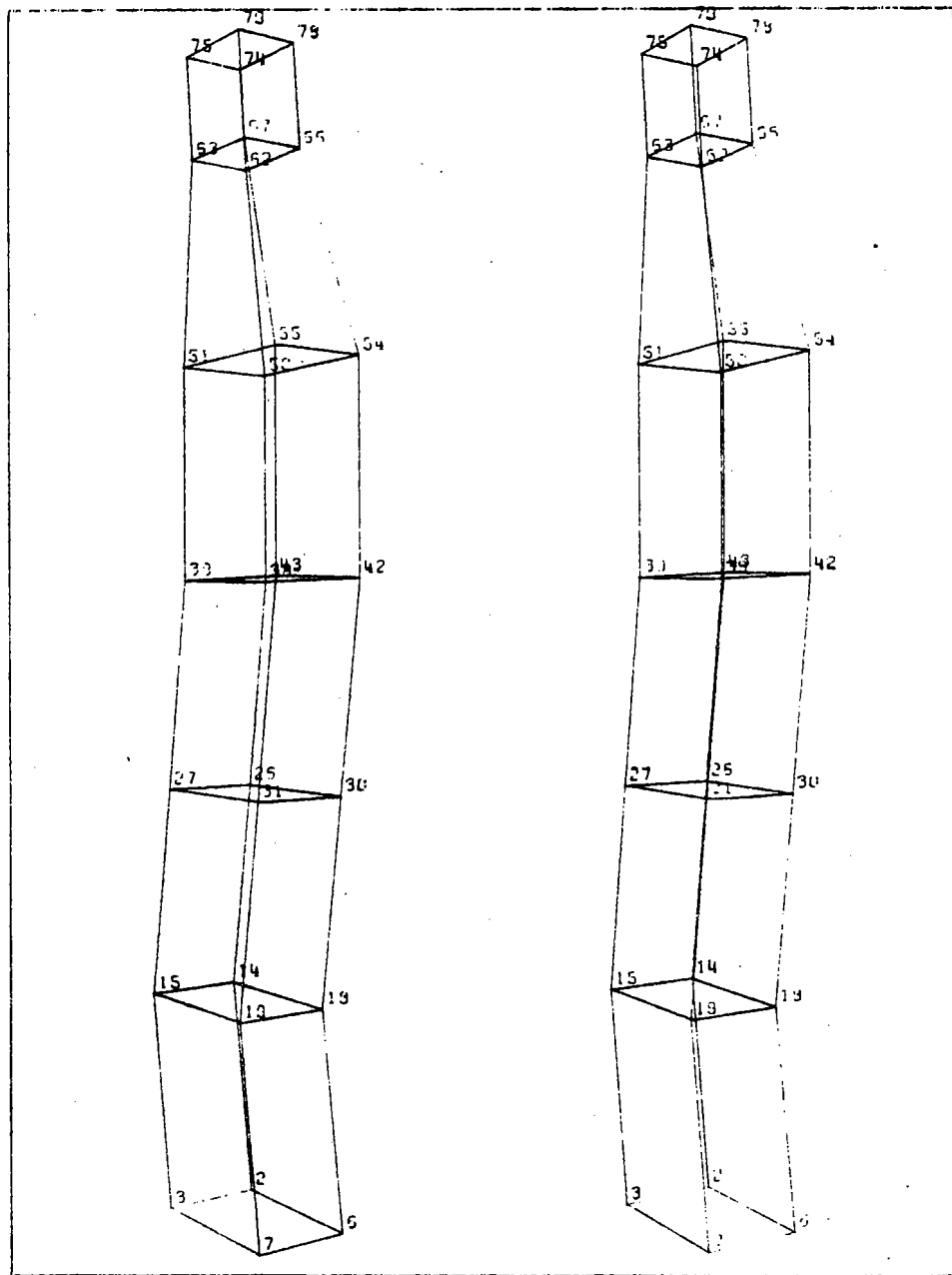


Figure 2. Stereographic drawings of the fixed model vertebral column.

stiff unless special provisions are made for free pivoting. The finite element representation may then either include low friction pads as structural elements or may be reassigned mechanical property values to assure that the overall mechanical properties of the finite element spinal column approximates those of the real spinal column. Other elements must be added to represent other portions of the torso before the system mechanics are evaluated.

The dimensions of the spinal column are chosen first to satisfy the overall body dimensions as represented in Table 2. Second, a number of elements are chosen to represent the flexibility of the spinal column but with a minimum of data and variables to be handled in the computer analysis. Thus the 24 individual vertebrae are not separately represented. The other portions of the body are represented by similar brick elements as shown in Figure 3. The addition of these elements allows the representation of shape and the provision of mass to simulate the actual body mass and to provide for the inertial moments of the body.

In addition to the brick type element a variety of others may be conceived and employed. By using different element types in the analysis it may be possible to effect an economy in calculation especially in the structural analysis part of the program. A group of typical elements is shown in Figure 6. Only one type of element has been employed in the programming to date on the body-head-helmet system studies in this research. However, dynamic analysis has been performed using a composite element simulation in which the body is represented by a column of beam type elements supporting a pseudo spherical head. Dynamic simulation is described in a later section of this report.

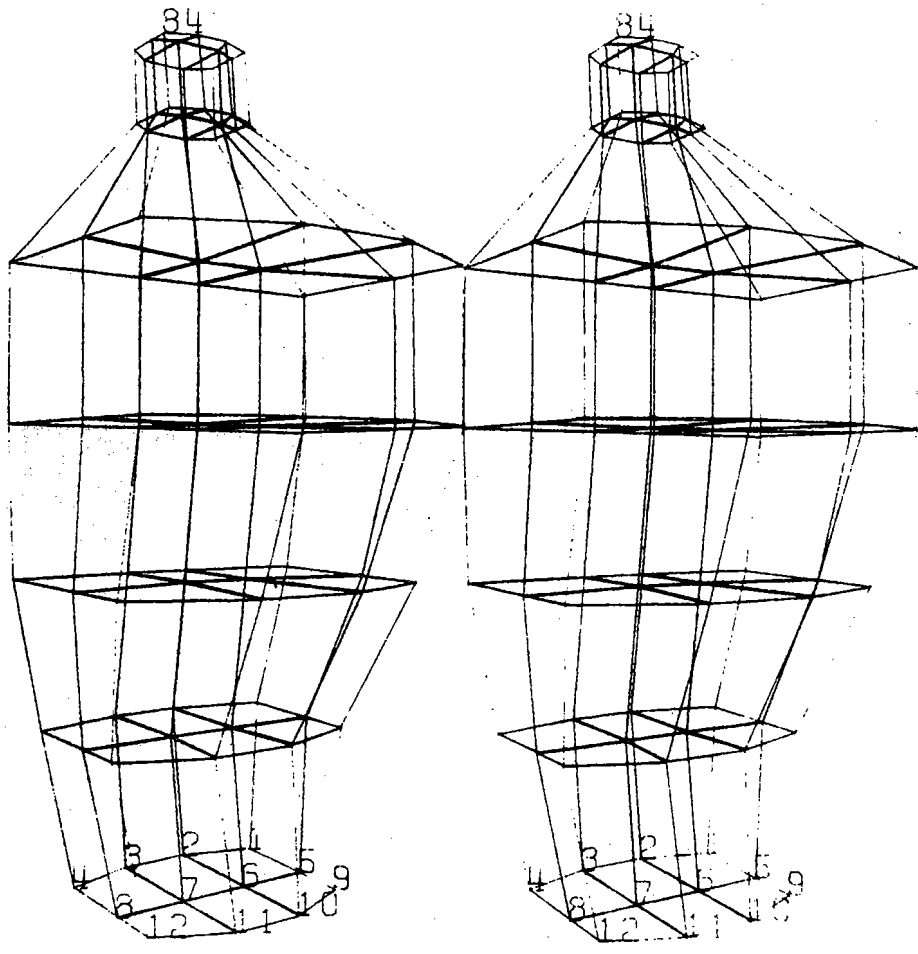


Figure 3. Stereographic drawings of the fixed model torso.

The term, finite element analysis, generally refers to structural analysis but in the broader sense includes other operations such as the study of mass distribution and inertial moment distribution, which may also be conveniently performed on the system of finite elements. Each of these will be briefly described in relation to their use in this research.

B. Stereographic Drawings

A number of the figures are computer drawn stereo pairs that provide a depth perspective. The left and right hand drawings are formed separately by projecting the nodal points from arbitrary projection points onto a viewing plane. The projection points are arbitrary with respect to distance and direction from the nodal point group but are related so that the two projected figures may be fused by the observer. The fusion may best be implemented with a stereo viewer or simply by training the eyes. This is aided by holding a hand or piece of cardboard in front of the nose and perpendicular to the drawing. It may be easiest to separately fuse the two sets of coordinate axes at the bottom of Figure 10 before attempting the entire figure. This fusion enhances detail, making it possible for many internal features to be distinguished that are otherwise obscure.

C. Inertial Properties

1. Nodal Points

The data is introduced into the computer in essentially four sets of statements. One set contains the coordinates for each nodal point specified relative to the same coordinate system. There also is

information relating to the degrees of freedom allowed for each nodal point. Figure 4 represents the information for one such nodal point.

2. Elements

Each element of the type employed in this study is defined by eight of these nodal points from the list. This arrangement is illustrated in Figure 5A with nodal points numbered in sequence. The connection array for the elements shown in Figure 5A is

1	2	3	4	5	6	7	8
---	---	---	---	---	---	---	---

For every element in the structure a connection array is entered into the program. An example is element no. 104 (see Appendix A) for which the connection array is

166	167	227	226	174	175	187	186
-----	-----	-----	-----	-----	-----	-----	-----

The finite element representation of the body-head-helmet system uses 382 nodal points and 204 elements. Element 104 which is listed above is also defined to be material type 2. All of this information is entered with the connection array. A third type of information entered into the computer is the values of other parameters such as materials properties and loading conditions and the fourth type of information is general instructions relative to the mode of computation to be performed. All of this data is stored in the computer in a way in which it can be readily accessed for use and reuse.

3. Centers of Gravity

The centroid of each element is determined by averaging each component set of coordinates. This is expressed in equations [1].

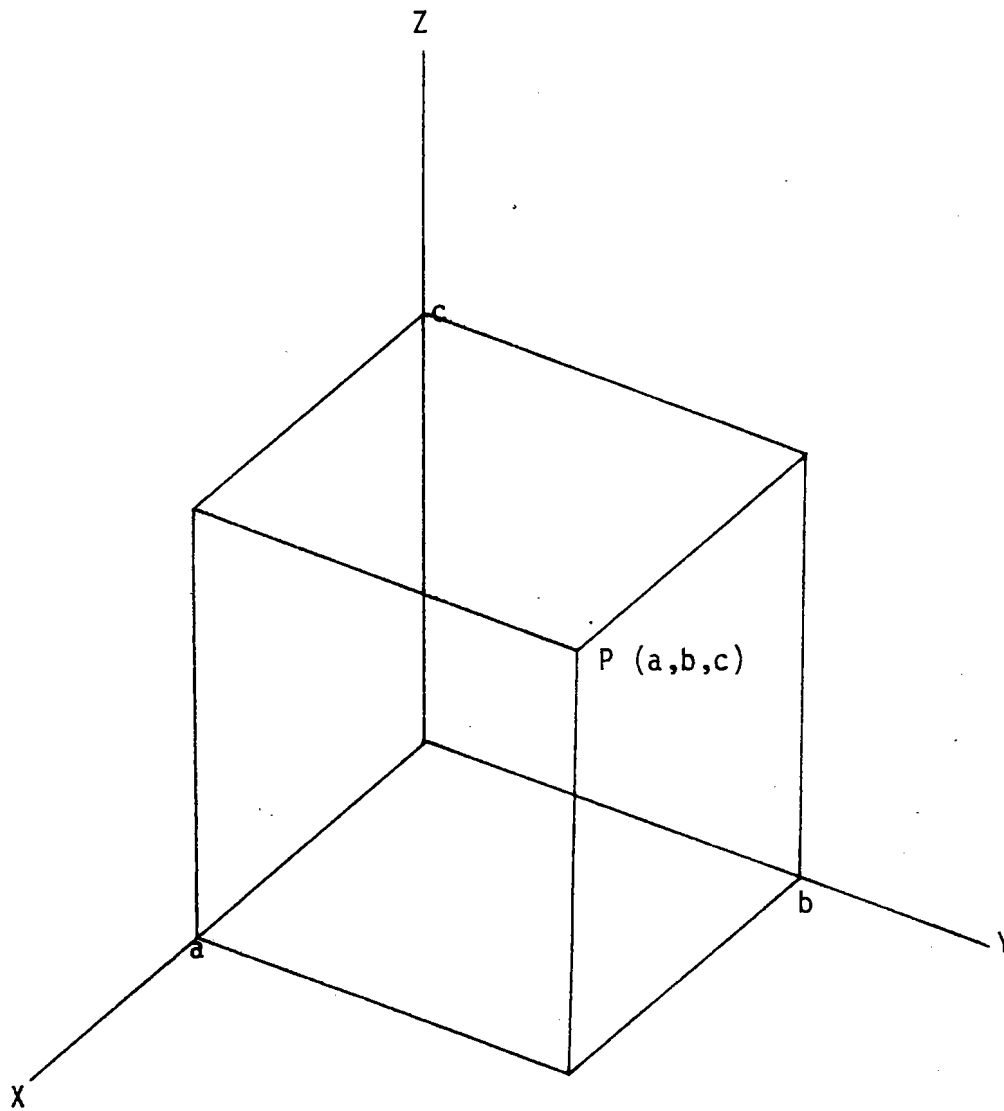
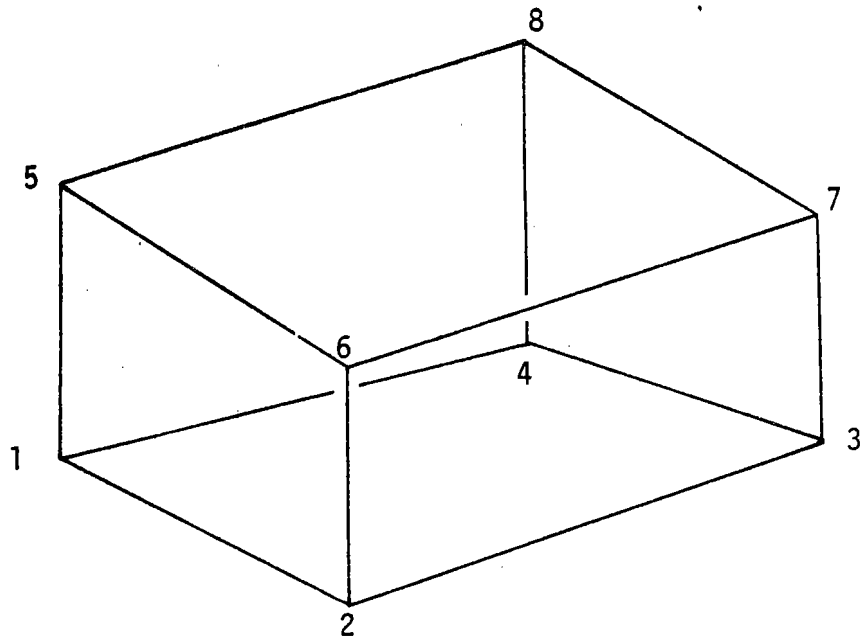
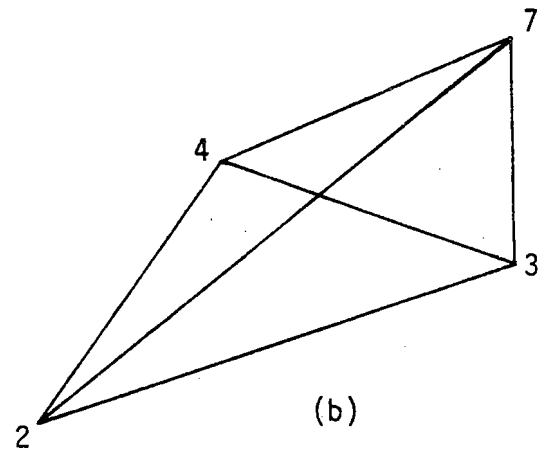


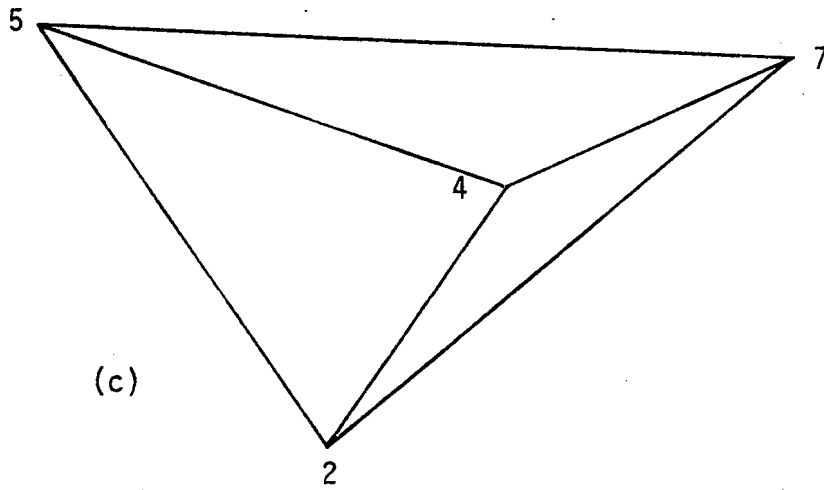
Figure 4. The coordinates of nodal point p.



(a)



(b)



(c)

Figure 5. The brick type element. a. Nodal points numbered sequentially from 1 through 8. b. Typical corner-type tetrahedron. c. Typical central tetrahedron.

$$x_c = \frac{\sum_{i=1}^8 x_i}{8}$$

$$y_c = \frac{\sum_{i=1}^8 y_i}{8}$$

[1]

$$z_c = \frac{\sum_{i=1}^8 z_c}{8}$$

The coordinates of the centroid are x_c , y_c , and z_c .

4. Element Volume

To facilitate computation, each element is subdivided into five tetrahedra as defined by the following nodal points referred to in Figure 5A.

1	3	2	6
3	1	4	8
8	1	5	6
6	3	7	8
5	2	7	4

The first four sets represent tetrahedra that are typified by the corner-type tetrahedron of Figure 5B and the last set is typified by the tetrahedron in Figure 5C.

Three non-planar edge vectors are defined for each tetrahedron with components corresponding to the differences between the corresponding coordinates of the nodal points. For example, the vector \vec{V}_{ij} is given by

$$(x_j - x_i)\vec{a} + (y_j - y_i)\vec{b} + (z_j - z_i)\vec{c} \quad [2]$$

where \vec{a} , \vec{b} , and \vec{c} are unit vectors along the x, y, and z-axes, respectively. The volume of each tetrahedron is then

$$\text{Vol} = \frac{1}{6} \vec{V}_{ij} \times \vec{V}_{ik} \cdot \vec{V}_{il} \quad [3]$$

for the tetrahedron of nodal points i, j, k, and l. The volume of the element is the sum of the volumes of its tetrahedra.

5. Element Mass

The materials property data provides densities for each materials type, and the mass of each element is calculated as the product of its volume and density.

6. Mass Moment of Inertia

The inertial moment is also computed from the tetrahedra of each element; each tetrahedron mass, volume, and centroid are computed and combined to yield the inertial moments about the tetrahedron centroid. These are then recomputed about the centroid of the parent element and combined to produce the element centroidal inertial moments. Each element moment is then recomputed to a corresponding moment about the element group centroid and these are combined for the final result. The details are listed in subroutine S1800 in Appendix C.

7 Element Group Properties

The group value for each of the above parameters is computed for a specified group of elements by accumulating the appropriate information following each element calculation. For example, group mass and volume are the sums of the individual element masses and volumes. The group centroid is found by accumulating the sum of the products of element masses and centroid coordinates, and finally dividing each sum by the accumulated mass. For example, Equation 4 illustrates the calculation of the element group centroid x-coordinate, x_c for a group of NL elements.

$$x_c = \frac{\sum_{i=1}^{NL} m_i x_i}{\sum_{i=1}^{NL} m_i} \quad [4]$$

m_i is the mass of the i th element, and x_i is the x-coordinate of its centroid.

D. Static Structural Analysis

The element is again the basic unit to which the structural analysis is applied. As originally formulated each nodal point has a position that is specified by its original coordinates. Under the action of new forces and dependent upon the mechanical characteristics of the materials of which the system is composed, the coordinates of each nodal point will probably change unless subject to some special constraint, generally termed "boundary conditions". As a result of these nodal point displacements each element will become distorted in shape and angles between

faces. The form of the new configuration corresponds to a satisfaction of the principles of detailed force (equilibrium conditions) balance at each nodal point and minimization of energy of the system. These relationships are ensured because of the nature of the process by which the element equations were derived.

1. Variables and Equations

In general, each nodal point requires the specification of three coordinates and hence contributes three degrees of freedom or three variables to the system. The static configuration used here has a total of 1146 degrees of freedom, or there are 1146 unknowns to be determined. However, since 15 boundary conditions are specified, only 1131 variables remain to be determined. Each element provides 24 equations to define the force at each node in each direction that is caused by unit displacement of each of the nodal points in a corresponding manner. Equations 5 represent this set of 24 equations.

$$\bar{F}_1 = \bar{S}_{11}\bar{d}_1 + \bar{S}_{12}\bar{d}_2 + \dots + \bar{S}_{124}\bar{d}_{24}$$

$$\bar{F}_2 = \bar{S}_{21}\bar{d}_1 + \bar{S}_{22}\bar{d}_2 + \dots + \bar{S}_{224}\bar{d}_{24}$$

$$\begin{matrix} \cdot & \cdot & \cdot & \cdot & \cdot \\ \cdot & \cdot & \cdot & \cdot & \cdot \\ \cdot & \cdot & \cdot & \cdot & \cdot \end{matrix} \quad [5]$$

$$\bar{F}_{24} = \bar{S}_{241}\bar{d}_1 + \bar{S}_{242}\bar{d}_2 + \dots + \bar{S}_{2424}\bar{d}_{24}$$

Where \bar{F}_i , \bar{S}_{ij} and \bar{D}_j represent force, stiffness and displacement components relative to the coupling between the i and j nodal points. The

line above the symbol relates the variable to the element rather than to the system as a whole. The group of equations for each element can be written in simplified matrix notation as

$$\{\bar{F}\} = [\bar{S}]\{\bar{d}\} \quad [6]$$

The entire system of elements is described simply by a similar matrix equation

$$\{F\} = [S]\{d\} \quad [7]$$

Where the system stiffness matrix $[S]$ contains all of the individual element stiffness matrix terms. There are 1131×1131 or 1,279,161 values to be set in the static analysis problem referred to here.

2. Solution and Results

The unknown displacements are found by inverting $[S]$.

$$\{d\} = [S]^{-1}\{F\} \quad [8]$$

The force can be specified in many ways such as concentrated or distributed surface loads, residual stresses, etc. Equation 8 represents a critical step in the solution procedure. The inversion of matrix $[S]$ represents an overwhelming number of arithmetic operations. This step, perhaps more than any other, dictates the use of a modern high-speed digital computer.

The strain components are calculated for each element from the original and new coordinates. This is performed according to the definition of engineering strain. The stresses are calculated using the

stress-strain relations that apply for the material. Finally, stored energy and other derived parameters are calculated from these results.

3. Accuracy and Execution Time

If the elements are so planned that the parameters of each are a good approximation of the average real value in the related region of the original subject, and if the variation in the calculated displacement field is not great through the region, the overall calculation will produce accurate results. These can easily approach a fraction of a percent. However, computer time and capacity may prove to be the overriding consideration. Accuracy can be improved by:

1. Increasing the number of elements used, and hence reducing element size.
2. Limiting the forces used if the structure is deformed beyond true elastic limits.
3. Changing element type or computational procedure in order to correct the above problems.

It is frequently desirable to limit the number of elements in the structure. One static analysis run of the fixed (382 nodal point, 204 element) structure requires approximately one hour of active computing time and four hours resident time in the machine, occupying approximately 60% of the available operational space. It is possible to improve these operating parameters and even to simultaneously refine the mesh size in selected regions.

E. Dynamic Structural Analysis

Equation 7 is the basis of the static analysis and Equation 9 is the related equation for a dynamic analysis.

$$[M]\{\ddot{d}\} + [K]\{\dot{d}\} + [S]\{d\} = \{F\} \quad [9]$$

Where $[S]$, $\{d\}$ and $\{f\}$ are the same as defined before, $[M]$ and $[K]$ are mass and damping coefficient matrices respectively and $\{\dot{d}\}$ and $\{\ddot{d}\}$ are velocity and acceleration vectors respectively. Again there are solution procedures similar to (8) but involving the solution of differential equations, frequently involving integration. Hybrid computers are suited to this type of analysis, but equipment and procedures have not yet been developed to fully realize this potential.

Two solution approaches are possible. One involves the determination of the natural frequencies in the system and calculating the displacement contribution from each mode. The other is by direct integration. Each method allows the action to be applied as either:

1. A time varying load which may be in the form of concentrated or distributed loads in all of the various manners that are allowable for the load determination under static loading conditions.
2. A time varying ground motion which can lead directly to the evaluation of inertial behavior of the system.

A great amount of flexibility is allowed in terms of the specification of the load variation. For the ground motion specification it is possible to program the acceleration profile, including the onset rate, peak acceleration and the rate of drop off.

The results of the solution of Equation 9 are in the form of displacements, stresses, etc. similar to those obtained through the static

analysis but are determined at individual time steps, thus allowing the tracing of time histories. These are illustrated in the fourth section of this report.

F. General Comments on Computer Operations

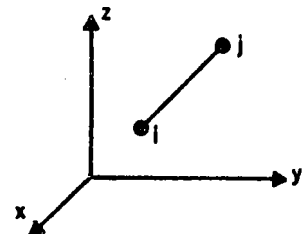
Service programs were written to generate nodal points and connection arrays. The system used in the static analysis was generated semi-automatically and is fixed in form. It therefore lacks flexibility. It is not easy to reduce the element size maintaining the same configuration volume and total mass. The near spherical configuration used to model the head, inner liner, and helmet shell was completely computer generated and hence is adaptable to studies involving the variation of mesh size. Other service programs were written to compute the mass distribution parameters described above and to make projective drawings and other special representations to aid in the evaluation of the results. These programs are listed in Appendix C.

The structural analysis program, SAP IV (2) was purchased to be incorporated into the system of programs. Both the program in tape form and the documentation are available from the University of California (15). The following two quotations from the documentation manual and a letter of transmittal received with the program explain the conditions for its use. "The development of the computer programs SAP including SAP IV has been supported by many organizations during the past years. The final phase of development and documentation of SAP IV was sponsored by a grant from the National Science Foundation." "The distribution of SAP IV is unlimited, but the program is not to be used for direct profit without authorization. In other words, royalty or development charges

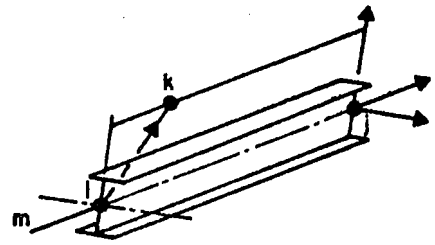
are not allowed, and the program should not be sold. However, please feel free to give the program to other organizations at the cost of duplication, mailing and handling."

There are a number of other structural analysis programs that are commercially available and that might be used. SAP IV, however, provides a number of convenient features for the analysis such as the flexibility and specification of forces and ground motions and includes 8 different element types as shown in Figure 6. Many of these elements may be combined in one configuration to improve the economy of operation or to provide some other benefit. Also, having performed a structural analysis on a given configuration, it is relatively simple to make additions of other elements to evaluate, for example, the effect of peripheral equipment on the mechanics of the system. Finally, this program, by means of the nature of its design, provides for the addition of other elements that may be developed to meet specific needs.

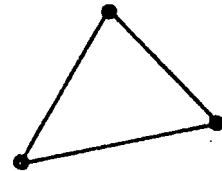
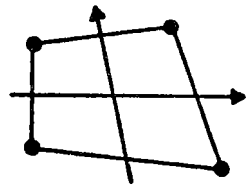
It is possible to run the same sample configuration by different modes of analysis for purposes of comparison. The analyses that are presented in the following sections are simply a small sampling of those that may be performed. Once formulated, a system of computer programs for finite element modeling is a very flexible and easily controlled design tool.



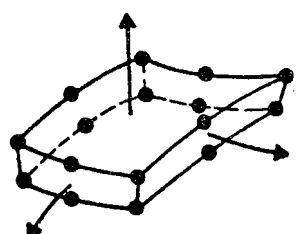
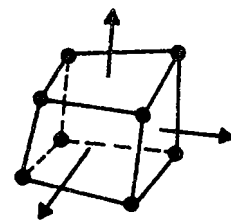
a. TRUSS ELEMENT



b. THREE DIMENSIONAL BEAM ELEMENT

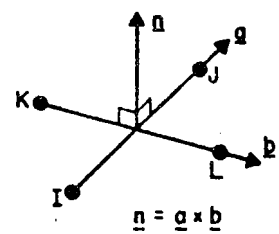
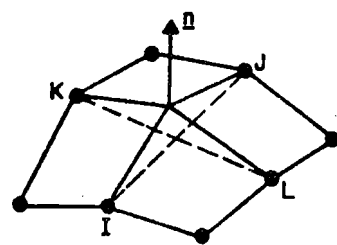


c. PLANE STRESS, PLANE STRAIN AND AXISYMMETRIC ELEMENTS

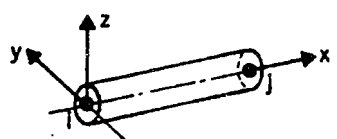


d. THREE DIMENSIONAL SOLID

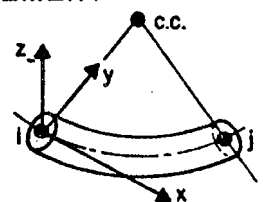
e. THICK SHELL ELEMENT



f. THIN SHELL AND BOUNDARY ELEMENT



TANGENT



BEND

g. PIPE ELEMENT

Figure 6. Element Library of SAP IV.

III. RESULTS: STATIC ANALYSIS

A. System Mechanics

1. Linear Deformation

Static analysis provides information about the shape and dimensions of a mechanical system under the action of various forces. When a force is applied to the surface of an object it deforms until its internal forces oppose and balance the external force. As the external force is gradually (slowly) applied the system may be assumed to pass through a continuous sequence of force balance states. For a system defined to have linear elastic properties, the magnitude of each deformation mode is proportional to the magnitude of the applied force. This is true as long as the accumulated changes do not make an appreciable change in the dimensions or shape of the structure. Also, in a linear elastic system the deformations resulting from different external forces can be superimposed directly. If the deformations are so extensive that linear elastic analysis does not apply, a different mode of analysis must be used.

2. Relationship to Dynamic Loading

Under dynamic loads, as are encountered in vehicle crash situations, the kinetic energy of the system contributes to the deformation. A method of comparison is through the mechanical work in the system. The work of deformation in the dynamic system is calculated as the equivalent of the kinetic energy of the system prior to the moment of impact. This correspondence is reasonable as long as the velocities involved do not approach any of the velocities of sound through the system. The specific

assumption made is that the forces and displacements used in calculating the work of deformation are average, steady state values for the system. Kinetic energy is the product of one half the mass times the square of its velocity, assuming that the mass is brought to rest. The mass is of those portions of the system that are affected.

$$E_r = \frac{1}{2} mv^2 \quad [10]$$

The work, or energy of deformation, E_p , in the static case is the product of the force, P , times the distance it moves, $\Delta\ell$, summed over every part of the system, for each deformation mode. For the linear elastic system studied here this is given by

$$E_p = \frac{1}{2} P\Delta\ell \quad [11]$$

which is illustrated in Figure 7. Thus it can be reasoned that the maximum possible deformation can occur if the kinetic energy is transformed with maximum efficiency. This does not take sequential changes into consideration but provides a useful approximation for events that do not occur at velocities approximating the velocity of sound. It provides an upper limit for the determination of the deformation that can occur under these conditions.

B. System Formation and Characteristics

1. Dimensions

A specific three dimensional configuration was formulated to represent the torso, neck, and head with a helmet consisting of a relatively thin spheroidal shell and an inner liner. The body portion of the system was described in Section III A and shown in Figure 3.

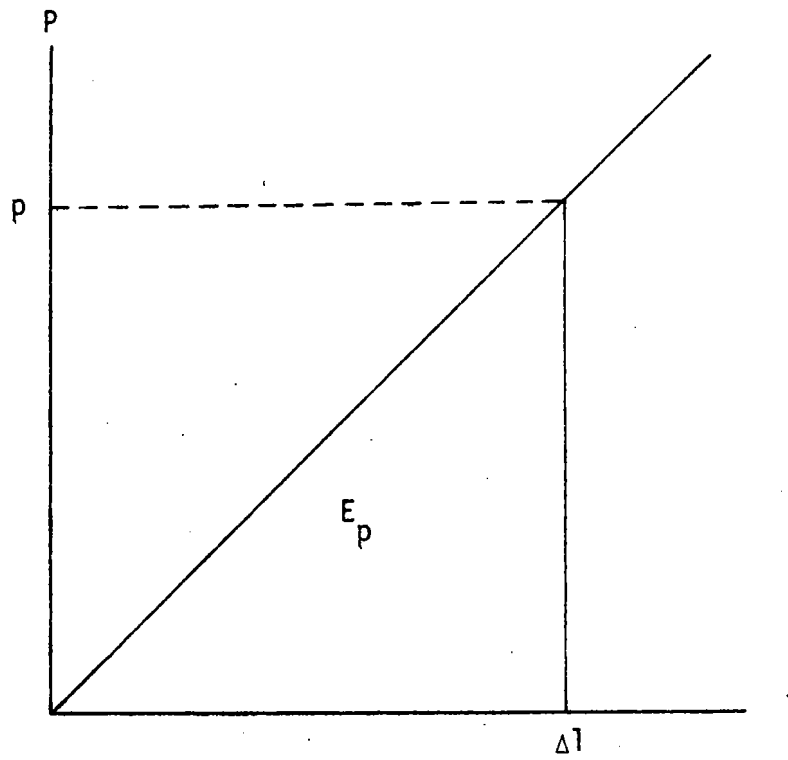


Figure 7. Materials Properties

The helmet shell, which is shown in Figure 8 was generated separately and added to the system. It is hemispherical except for the positions of four nodal points, at the front edge on each ear cover, and for the layer at the bottom edge in the back. There is also a small opening on each side corresponding with the positions of the ears. It is slightly over one centimeter in thickness.

The inner liner is shown in Figure 9. It is represented by a set of elements formed by making an analytical connection between the inner surface of the helmet shell and corresponding near nodal points on the skull. This was performed by adding a connection array statement for each inner liner element using the nodal point numbers of the skull and helmet shell surfaces.

2. Mass

This configuration provides a single grid. The structure was generated semiautomatically and is of fixed form. Elements of the system are classed into seven groups that allow the assignment of materials properties to adjust mass distribution and total weight in the different parts. The overall size and shape parameters correspond to those of the Automotive Safety Committee (1) and Ewing and Thomas(4). The density values are adjusted primarily to provide the desired total section weights. These values are listed in Table 2. This necessitated the assignment of unreal density values to some of the elements. The assigned materials property values are listed in Table 3. Improvement in this aspect of the simulation requires the use of more elements of smaller size and possibly special shapes. The agreement between body

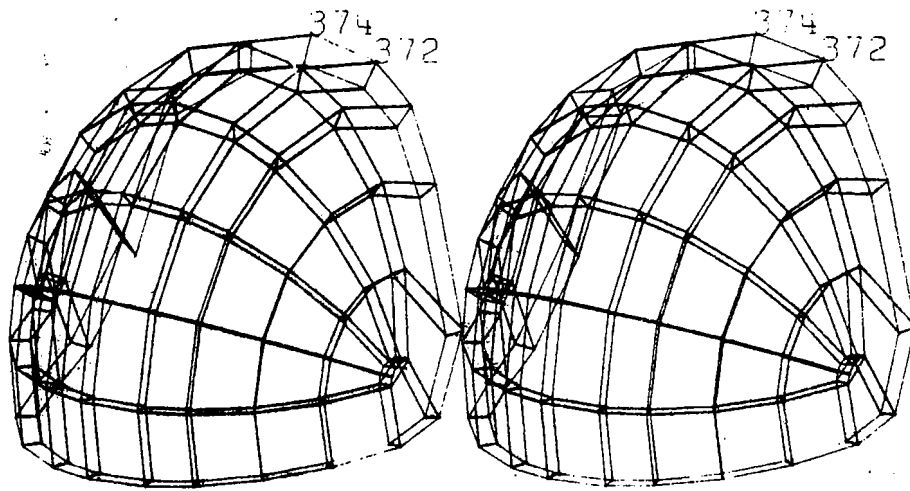


Figure 8. Helmet Shell

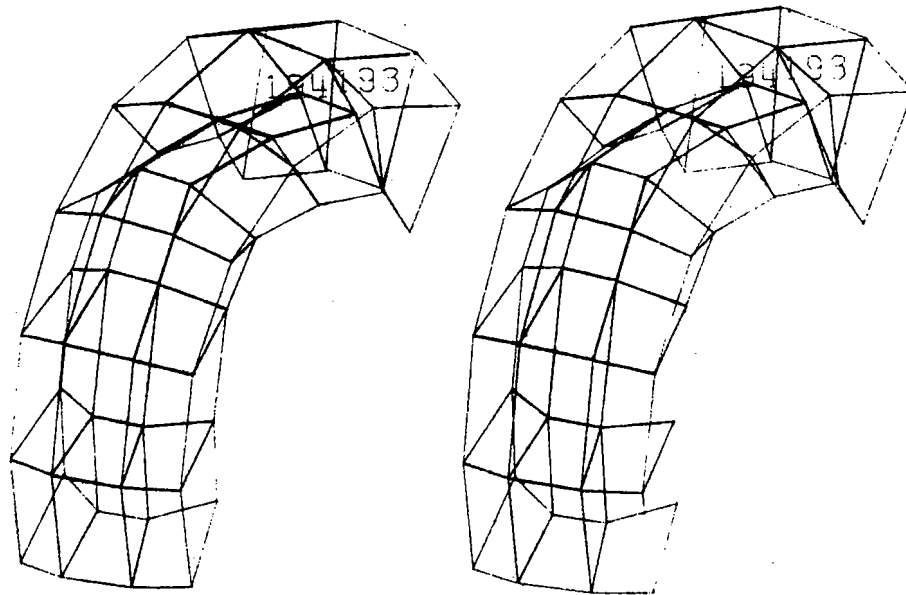


Figure 9. Inner Liner

TABLE 3
 MATERIALS PROPERTIES ASSIGNED IN THE FIXED
 BODY-HEAD-HELMET SIMULATION

Material Number	Description	Youngs Modulus (MPa)	Poisson Ratio	Density (g cm ⁻³)
1	Skull	4.52×10^5	0.3	1.47
2	Brain	2.83×10^1	0.3	1.05
3	Helmet Shell	2.83×10^4	0.3	1.75
4	Inner Liner	$0.6894 - 0.6894 \times 10^4$	0.3	0.06
5	Flesh	2.83×10^3	0.3	1.00
6	Spine	4.52×10^5	0.3	3.01

and model sectional weights and centroids is good with respect to the appearance of the geometric correspondence. The ultimate evaluation will depend upon other measurements such as moments of inertia. The total model, including the body, head, and helmet, is shown in Figure 10.

3. Inertial Moments

The inertial moments can be calculated for any group of elements or for the entire system as described in II C. Since the fixed model was established to represent a "typical" person, the moments were determined for sections through the torso in a manner similar to that studied by Liu and Wickstrom (11) on cadavers. The correspondence is only approximate, since the cadaver slices corresponded to vertebral sections, T5, T6, etc. (see Figure 1), and the simulation provides only six layers to correspond with the torso and neck. Nevertheless an examination of the radiographs (11) showed that the correspondence between layers might be close to that listed in Table 4.

The masses of the cadaver and simulation slices, however, differ considerably. Liu and Wickstrom clearly show differences between cadavers and living bodies; in fact, evaluating these and body inertial properties are the objectives in their paper. Table 4 lists the masses of the layers in the simulation and of the corresponding cadaver slices. The ratio of the two masses is 8.4 which indicates that not only are the materials different but the distributions are different. Table 4 also shows the inertial moments of the cadaver slices and the simulation. There is a large variation here too.

A calculation was made of inertial moments corrected for section weight. The cadaver moments were scaled up in proportion to the

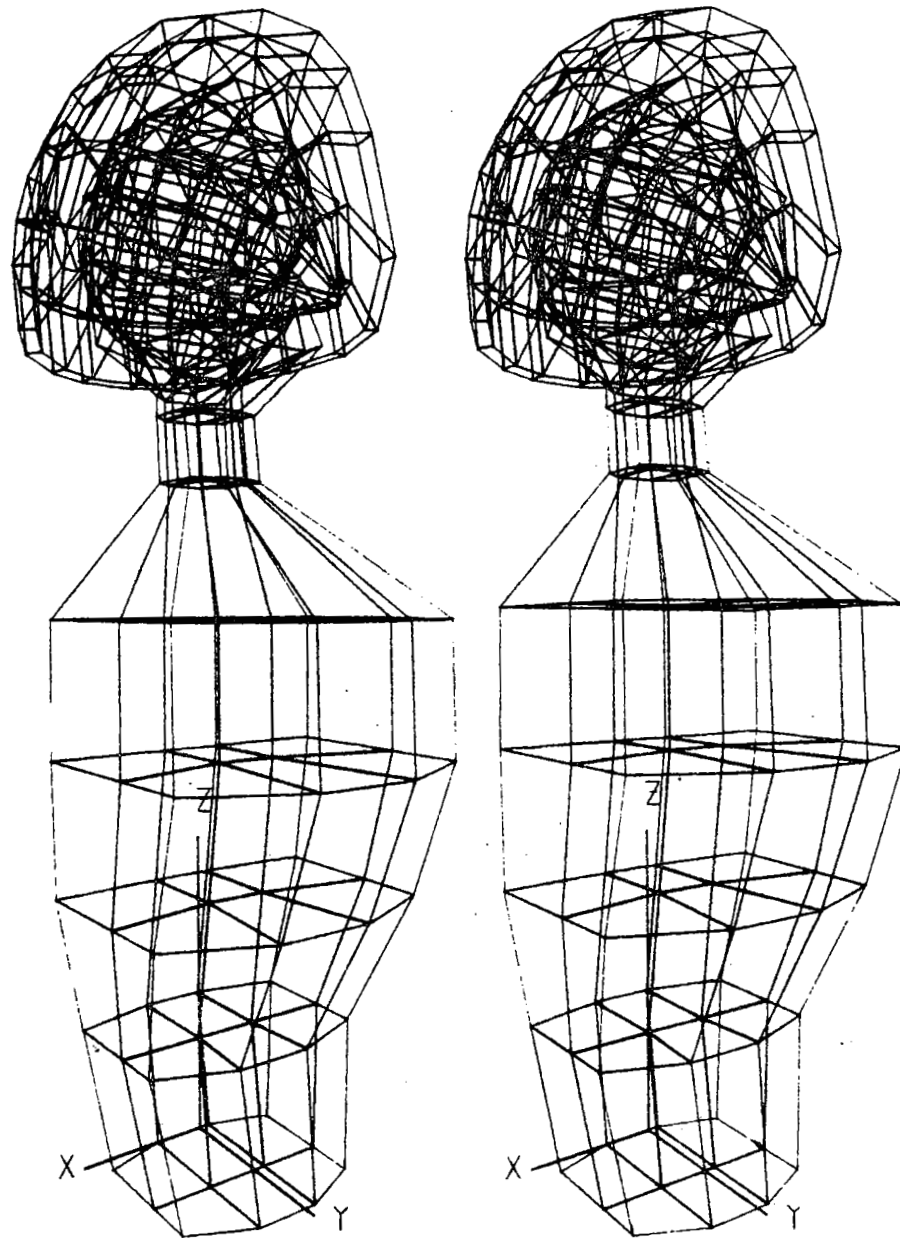


Figure 10. Fixed Model of Body-Head-Helmet System with C-ordinate Axes.

TABLE 4
INERTIAL PROPERTIES OF SECTIONS OF THE TORSO

Section*	Mass (kg)	Inertial Moment (kg cm ²)		
		I _{xc}	I _{yc}	I _{zc}
T1-T2+	0.2032	12.95	2.36	24.65
31-36	0.312	2.20	1.91	1.87
T3-T6+	0.3834	38.05	11.95	48.63
25-30	2.435	71.28	69.62	34.11
T7-T10+	0.4512	40.04	19.33	56.10
19-24	5.041	204.13	244.21	344.47
T11-L1+	0.4373	34.37	18.52	50.80
13-18	4.634	173.27	212.88	289.15
L2-L3+	0.3476	27.95	13.90	38.24
7-12	3.444	101.04	126.10	150.17
L4-L5+	0.3696	29.27	13.61	39.09
1-6	2.552	65.15	69.71	73.27
Increase of Scaled Value (%)				
Average		276.08	20.56	463.33
Standard Deviation		263.35	37.64	720.33

* The indicated combination of cadaver slices or the layer of elements, as marked.

+ Data of Liu and Wickstrom (11).

difference in mass between the corresponding sections as identified here. The percent increase of each scaled moment in relation to the corresponding simulation moment was calculated (but not listed). As an example, referring to Table 4, $I_{xc} = 12.95 \text{ kg cm}^2$ for T1-T2 and is scaled to a value of 19.88 kg cm^2 which corresponds to an increase of 803.64% relative to $I_{xc} = 2.20$ for simulation elements 31-36. The average value and standard deviation for each type of moment is listed at the bottom of each column of values. The basic differences between the model and the cadaver are due to the lack of mass distribution detail. The inertial moments can be directly adjusted for comparison. If the weights and shapes are similar, the inertial moments can be compared. I_{yc} compares well over the full set which indicates that the centroid of both systems lies on the Y-axis which is a line of near symmetry. The consistently high values in the other two experimental moments indicate that the mass of the cadaver is concentrated more to the front and back than in the simulation.

4. Stress Field

The system was anchored at the base so that no vertical deformation was allowed for nodal points 1 through 12, nodal point 2 is completely fixed and nodal point 5 was fixed to prevent rotation about a vertical axis. The coordinate system is shown in Figure 10. The surface force is applied, simultaneously, at two nodal points on the front of the helmet, horizontally backward (in the negative Y-direction). This set of boundary conditions is unsymmetric to a small extent and results in slightly unsymmetric displacements in otherwise symmetrically located regions of the system.

The sparsity of elements through any single section does not allow the generation of stress profiles. Instead Figure 11 presents a scale drawing of the midsagittal section with maximum normal stresses and maximum shear stresses represented for each element centroid on this plane. The length of each near horizontal arrow represents a relative magnitude of the maximum normal stress and the second arrow the maximum shear stress in that element. The lengths are proportional to the logarithms of the stresses. The materials type is listed in the circle. The direction and position of the applied forces is shown. Two applied forces of 6.22 N each were applied on nodal points 372 and 374, neither of which lies on the midsagittal plane but are symmetrically on opposite sides.

The plot shows that the general trend in the deformation may be followed by concentrating attention on a few nodal points and elements. These results are shown below.

C. Effect of Inner Liner Modulus

1. Materials Properties

The inner liner can be identified as the energy absorbing portion of the system. This may include the deformable suspension system with the foam material. The stiffness of this material or system of materials may be approximated by a single parameter for a first analysis. The deformation characteristics of a typical foam material are shown in Figure 12. The secant modulus may be chosen as the single, representative parameter over the expected range of deformation. This represents the ratio of stress required to produce an expected strain.

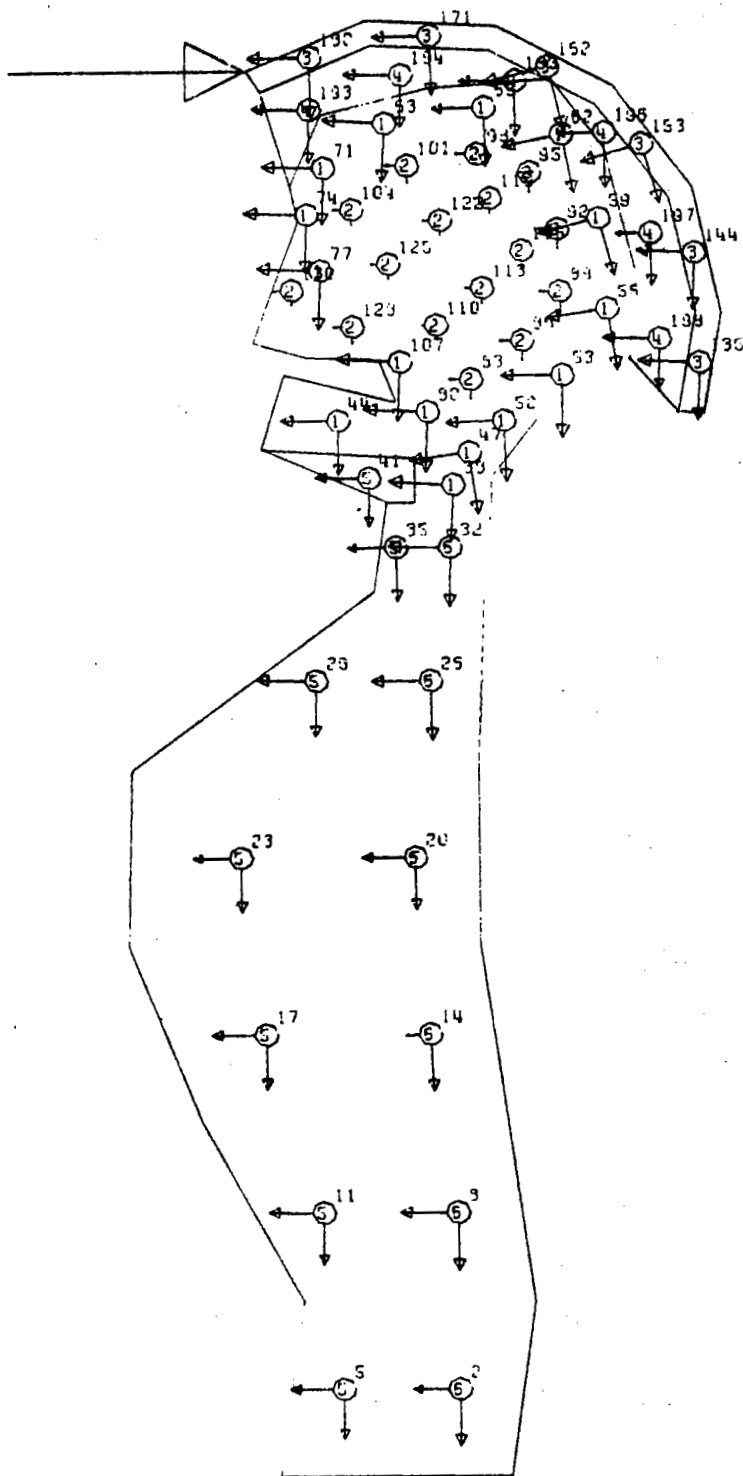


Figure 11. Midsagittal stress plot. Symbols located at element centers. Forward and downward directed arrows show direction and logarithm of magnitude of maximum normal and shear stresses, respectively. Materials type number is in center of octagon and the element is above and to the right.

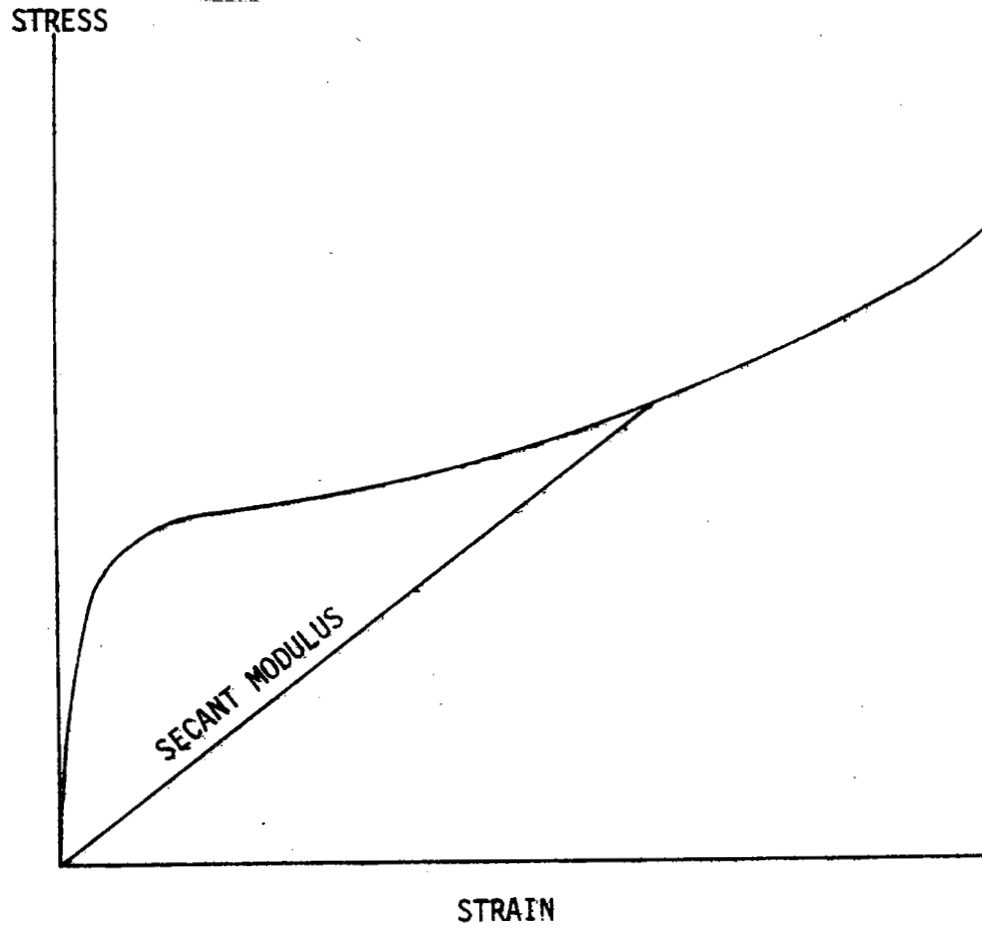


Figure 12. Schematic stress-strain curve for a typical inner liner material.

along an average, linear deformation path. The fact that real energy absorbing materials have non-linear characteristics is important and for the most faithful simulation elements with non-linear capabilities must be used in the simulation.

2. Displacements

With the above approximation in mind a series of simulation runs was performed for the system with all parameters fixed except that in each run a different inner liner modulus was used. The moduli ranged from .6894 to 0.6894×10^4 MPa (10^2 to 10^6 psi). This represents a broader range than that actually used and includes the level of stiffness in actual inner liner materials. The results are summarized in Figures 13 through 21. Each of these figures shows the variation of one measured parameter with liner stiffness. A trend is evident.

The helmet front displacement at the point of load application shows a monotonic decrease as the inner liner stiffness is increased. Figure 14 shows that the displacement at the front of the head has a different trend, increasing initially and passing through a maximum. The two opposing trends which produce this maximum are first the increase in nodal point displacement and force due to the more direct force transmittal through the stiffening inner liner and second, the decreased force in line because of the more effective force redistribution through the more rigid liner. The two curves in Figure 14 show the assymetric nature of the system. The scale on the ordinate shows that the difference in displacement between the two nodal points is very small. Nodal points 162 and 163 are on the front of the head in the region of the force application.

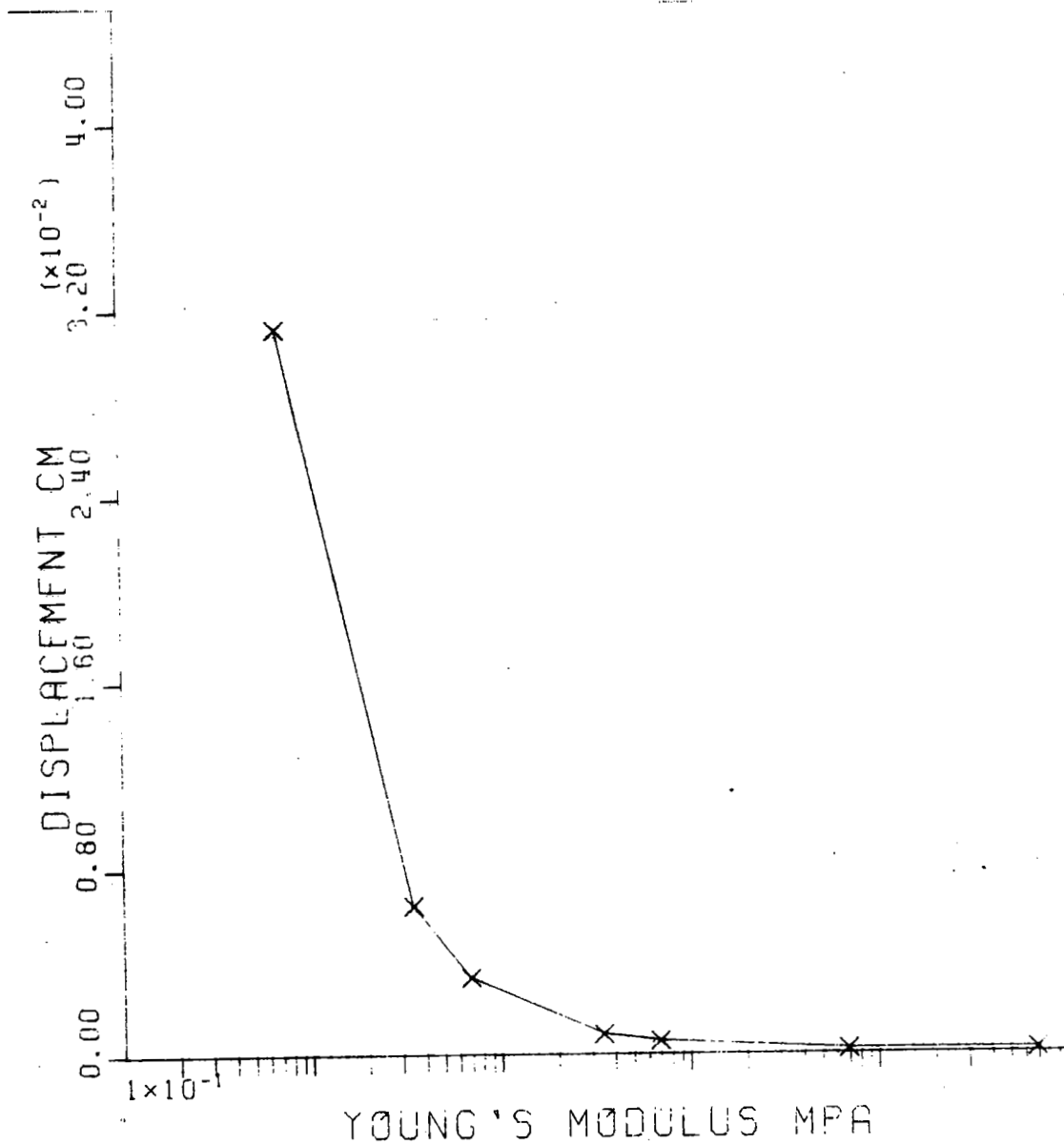


Figure 13. Displacement of the front of helmet at the point of static load applications (Nodal point 374).

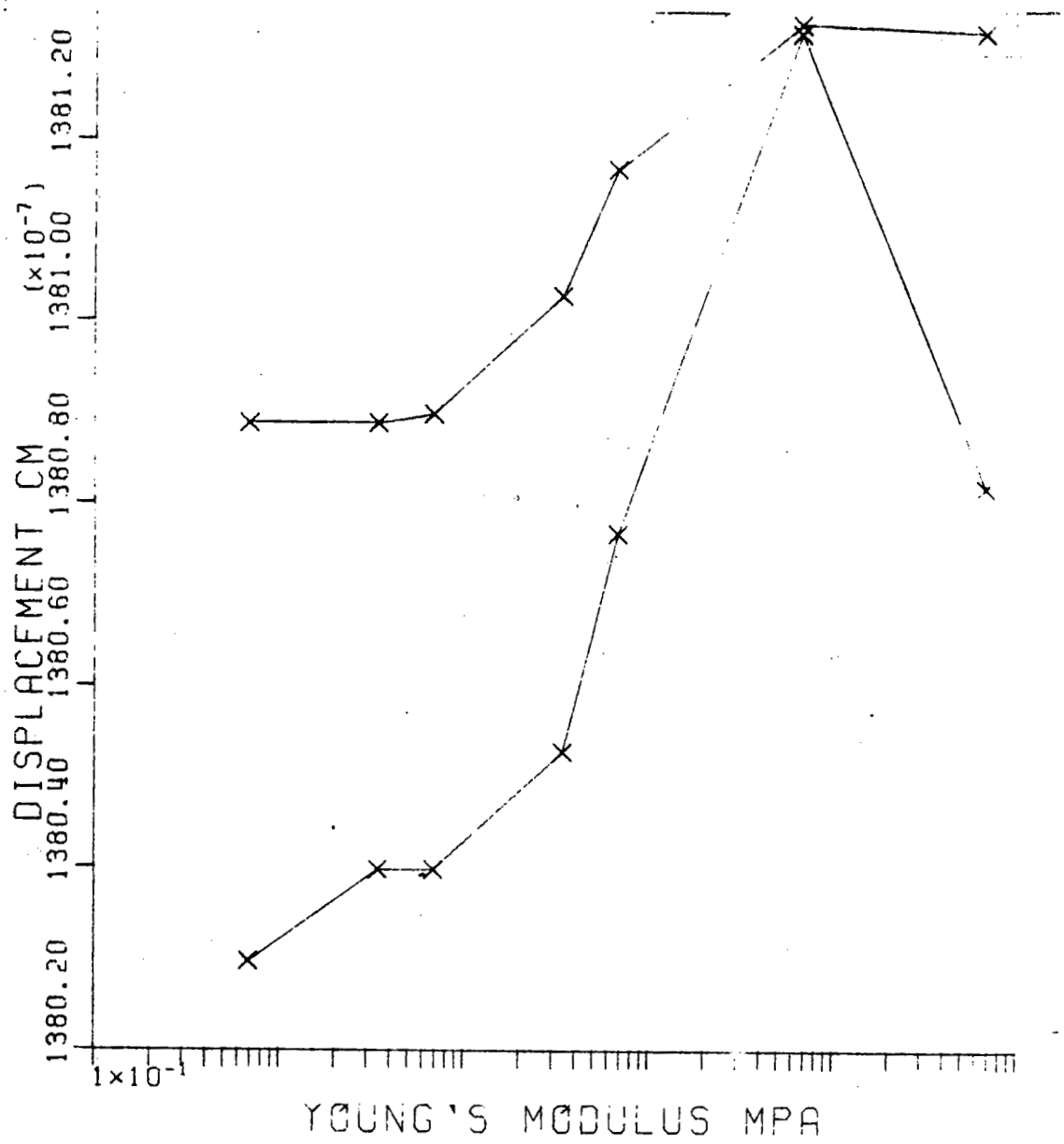


Figure 14. Displacement at the front of head (nodal points 162 and 163), approximately in line with the static load.

3. Skull Deflection

Figure 15 shows the original outline of the head along an approximately horizontal plane at the level at which the frontal force is applied. Curve B shows the displacement (exaggerated 10,000 times) for the most compliant inner liner and curve C is similar to B but represents the displacement for the least compliant inner liner. The exaggeration between C and B is 10,000,000 times. The results show relative head protection by the presence of a helmet and can be compared to the separate analysis of unprotected head deflection reported by Hardy and Marcal, (9) and stress (proportional to deflection) on the skull by Chan (3). Although the differences are exaggerated, the directions of the displacements are faithful to the analysis. Overall translation of the head is a dominant part of the displacement, but there is also a change in shape. The lack of boundary condition symmetry is reflected in the skull deformation.

The possible use of skull deflection information is in connection with evaluating the pressure that may result on the brain and in detecting the limits of loading that lead to skull fracture.

4. Stresses

The static analysis yields stress information which is of vital interest in terms of loss of consciousness and concussion. There is a growing body of evidence to relate these to shear stresses in the brain. Figures 16 through 21 summarize the stress results for elements 193 and 194 in the inner liner, numbers 68, 71, and 74 in the skull and 101 and 104 in the brain. Figures 16, 18, and 20 show the normal stress traces and Figures 17, 19, and 21 show the shear stress traces for the inner

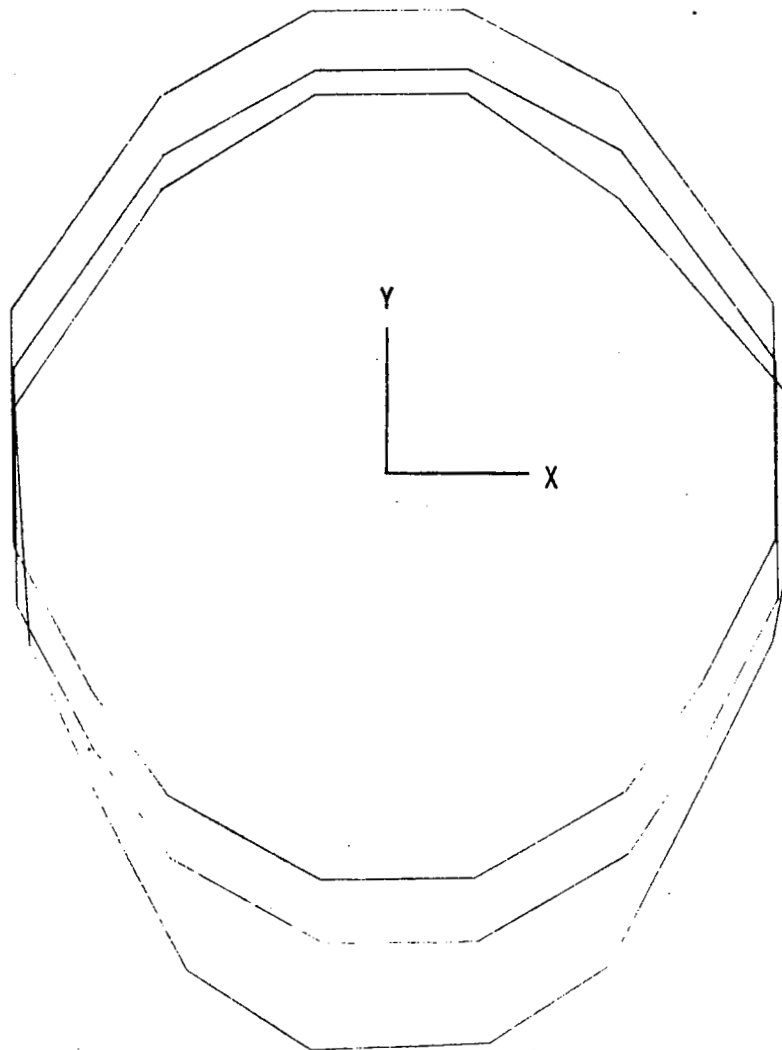


Figure 15. Skull deflection. This is a trace through nodal points on a transverse section at the level of the positions of static load application.

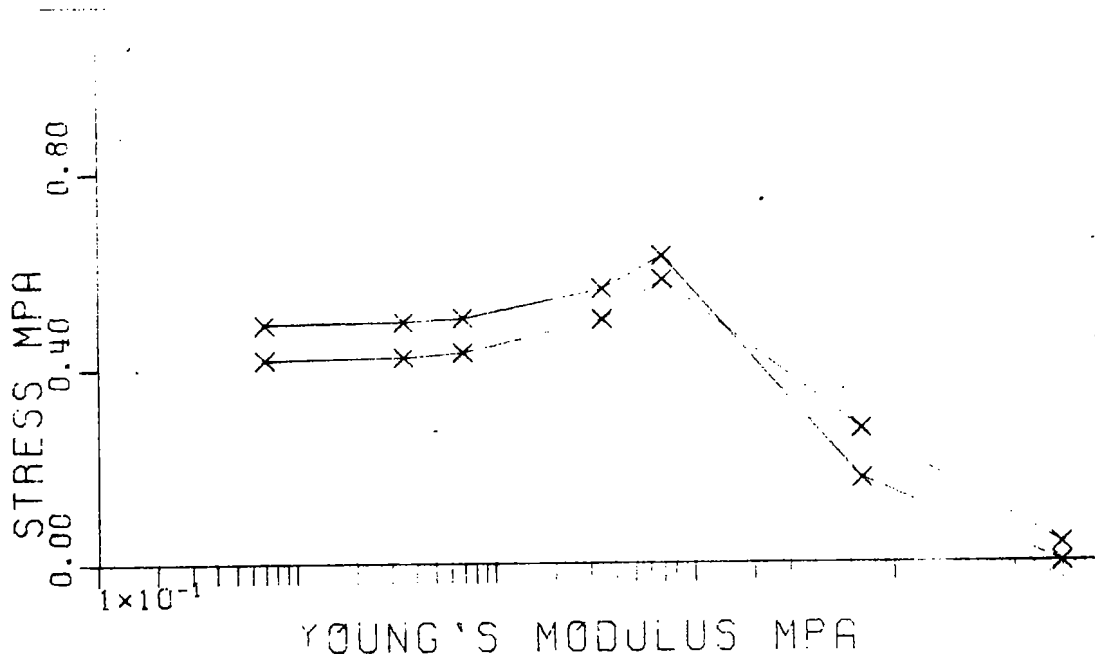


Figure 16. Maximum normal stress as a function of inner liner modulus in elements 193 and 194 at the front of the head in the inner liner.

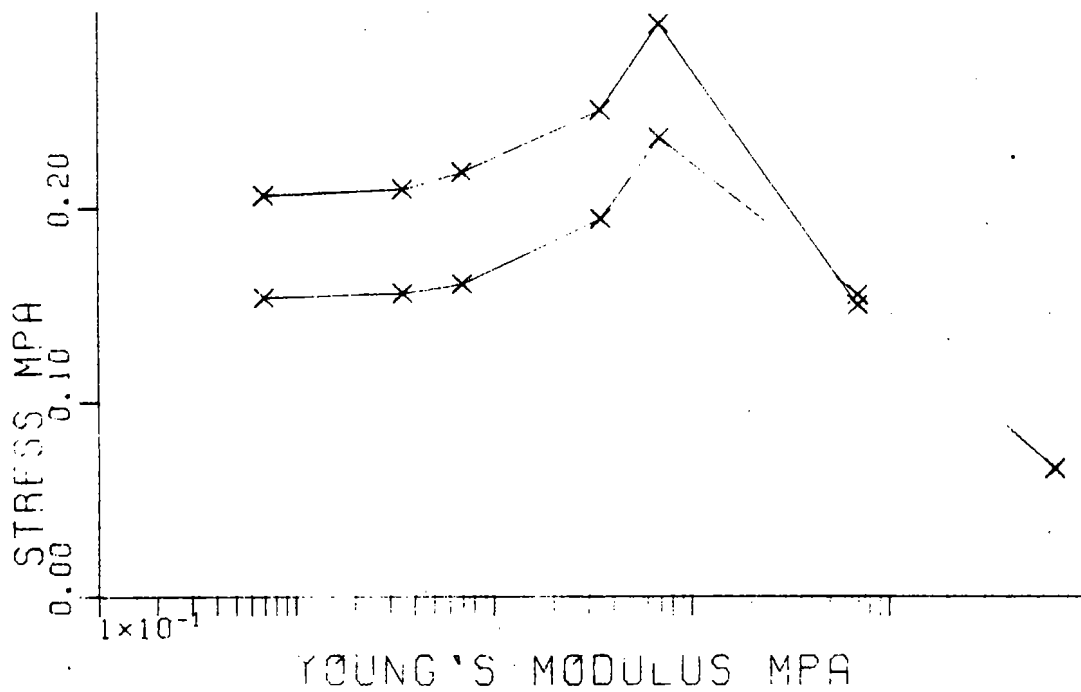


Figure 17. Maximum shear stress as a function of inner liner modulus in elements 193 and 194.

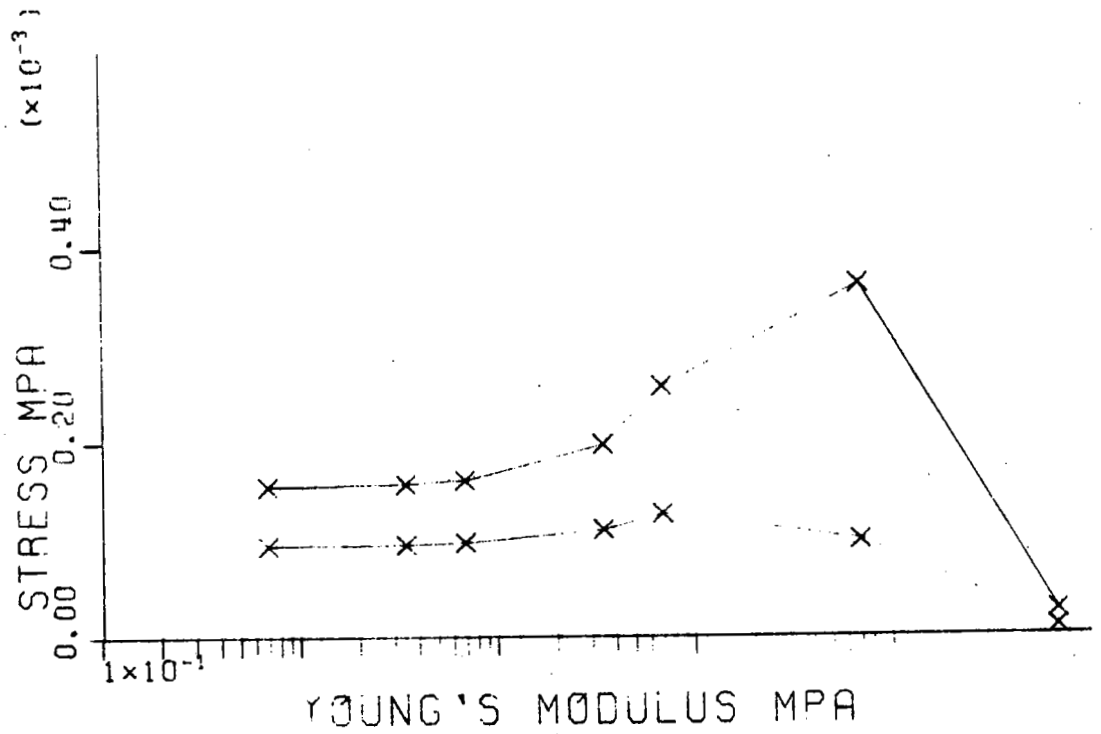


Figure 18. Maximum normal stress as a function of inner liner modulus in the brain (elements 101 and 104).

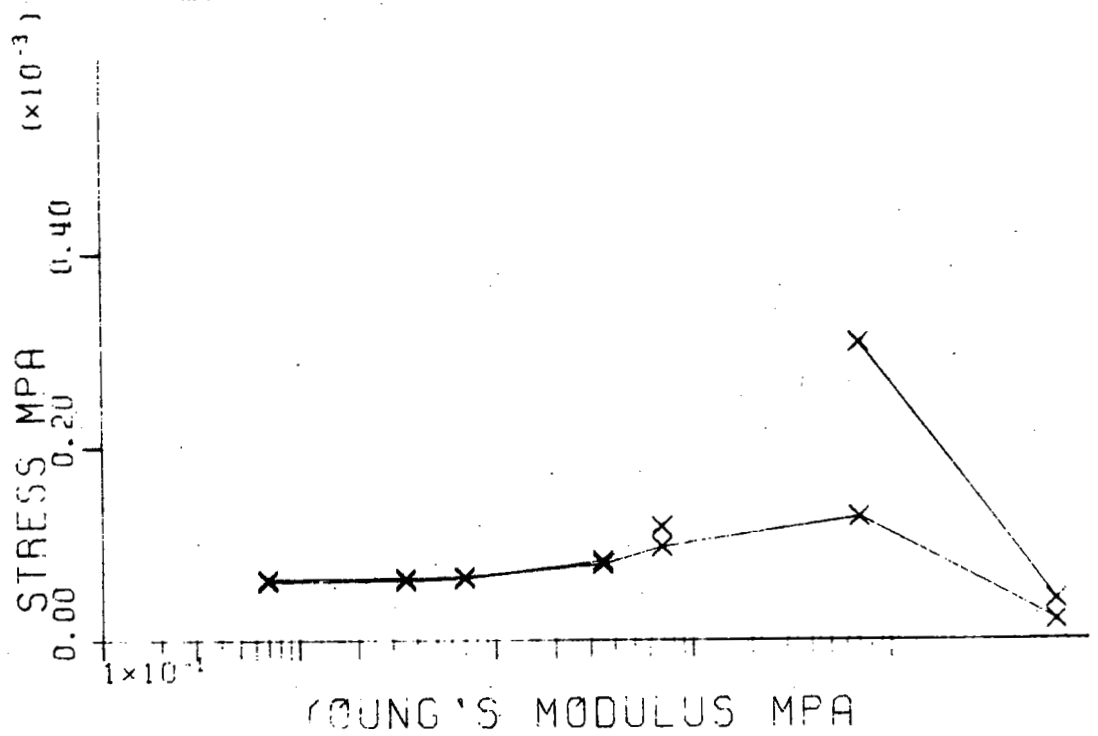


Figure 19. Maximum shear stress as a function of inner liner modulus in elements 101 and 104.

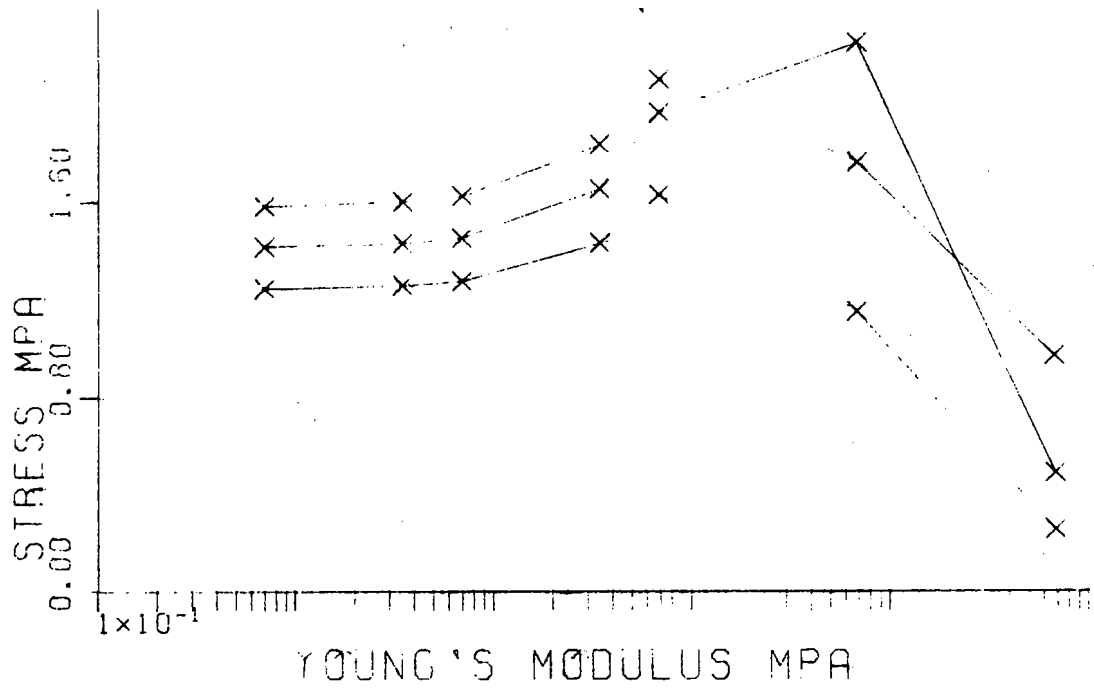


Figure 20. Maximum normal stress as a function of inner liner modulus in the skull in elements 68, 71 and 74.

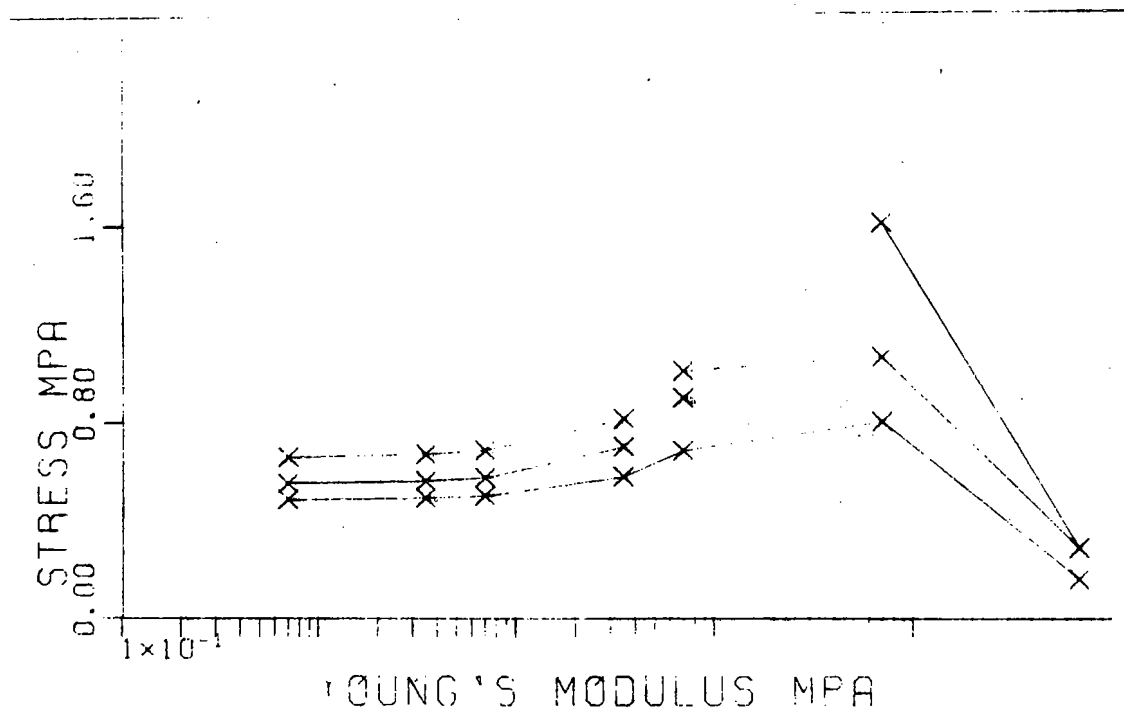


Figure 21. Maximum shear stress in elements 68, 71 and 74.

liner, skull, and brain elements respectively. These stress patterns show the maximum occurs in the range of 1 MPa inner liner modulus. The maximum shear stress occurs in the inner liner at a modulus value that is an order of magnitude lower. Again, the initial increase (as inner liner modulus is increased) in calculated stress can be attributed to the more direct action of the applied force against the in-line nodal points of the skull. However, as the liner modulus is further increased it attains a maximum followed by a stress reduction. It must be noted, however, that these peaks and reversals do not occur simultaneously. Thus the only trend indicated favoring head protection is to limit the modulus to low values. This is consistent with properties of foam materials now in use.

The multiple layer helmet (8) should be advantageous with a thin intermediate shell to distribute forces but without an overall stiffening effect. A parametric study of this design can be performed readily by computer simulation and checked experimentally with a limited number of helmets.

Examination of the configuration and the results indicates the need for refinement of the structure in a number of ways. Simplification in many regions is desirable. Grid generation totally by computer is mandatory. Other types of elements, such as the thick shell element of Figure 6, should be used for the helmet shell and the layered regions; and concentrated masses with three dimensional beam elements should replace large element groups where possible.

5. Work of Deformation

The 12.44N total force that is applied to the BHH system is orders of magnitude below forces of interest in crash simulation. However, each static analysis computation is representative of the reaction of the system to the applied forces. For any one configuration as used in a single run the reactions as evaluated by displacements of the nodal points and any other calculated parameters are proportional to the applied force. Thus, if the calculation were repeated for a force that is 100 times larger, the corresponding results would be 100 times larger. Table 5 lists the work performed by the applied forces in these computations. This work is calculated as the product of the applied force and the in-line displacement. The in-line displacements are shown graphically in Figure 13 as a function of inner liner modulus variations. Gurdjian (7) reports that 25 in lbs is critical for skull fracture. Using 20 in lbs for the helmet configuration with the stiffest inner liner which provides the least protection, the work ratio is 1.27×10^7 . This yields a force ratio of 3.56×10^3 . Thus if the applied force is increased to 22.1kN under these conditions, the impact will be critical. If this same force is applied to the system with the most compliant inner liner, only 1.52% of the work will be performed on the body. The inner liner will absorb more than 98%. The percent work absorbed by the inner liner is shown in the last column.

The force scaling factor (force ratio) can be applied to the normal stress and shear stress curves for an order of magnitude approximation of the stresses involved in a test situation that approximates usage.

TABLE 5
WORK OF DEFORMATION IN THE FIXED MODEL

Inner Liner Modulus (MPa)	Total Work (Ncm)	Work Ratio	Force (Displacement) Ratio	Inner Liner Work (%)
1.45×10^{-2}	.11979	19.2×10^5	4.38	98.48
7.25×10^{-2}	.02614	8.80×10^4	2.97	93.05
1.45×10^{-1}	.01444	1.60×10^6	1.26×10^3	87.42
7.25×10^{-1}	.00511	4.50	2.12	64.44
1.45	.00396	5.83	2.41	54.17
1.45×10^1	.00199	1.16×10^7	3.40	8.75
1.45×10^2	.00182	1.27×10^7	3.56	0

Shear stresses developed at the front of the head are of the order of 1 MPa, and in the brain of the order of 10^{-3} MPa. The interpretation of such values requires close correlation with experimental data.

IV. RESULTS: DYNAMIC ANALYSIS

A. Drop Test Simulation

A feature of SAP IV is the ability to apply dynamic analyses as explained in Chapter II. This was explored as a simulation of the drop test. The drop test involves a head form frequently cast in aluminum but more recently made with composites of various metallic and polymeric materials more closely representing the characteristics of the human head. The head form is raised to a predetermined height and released to accelerate under the action of the gravitational field and attains a maximum velocity, v_0 , at the moment of contact which depends upon this initial drop height. The relationship is given in Equation [12].

$$v_0 = \sqrt{2gh} \quad [12]$$

where g is the gravitational acceleration and h is the drop height. If the mass of the head form is m , the kinetic energy of motion is given by Equation [13].

$$\begin{aligned} \text{K.E.} &= \frac{1}{2} m v_0^2 \\ &= mgh \end{aligned} \quad [13]$$

This is converted to a potential energy of deformation with a total force F_m at some short time after contact.

$$\text{P.E.} = \frac{1}{2} F_m^2 / AE \quad [14]$$

As the maximum force is a function of drop height.

$$F_m = 2mAEgh \quad [15]$$

A is the area over which the force is distributed and E is the modulus of elasticity of the material.

Each particle of mass in the system must be brought to rest eventually and will, therefore, undergo a deceleration. The deceleration of each particle times its mass accounts for the force acting on that particle and this can be substituted into an appropriate equation to determine the new configuration of the system to balance out this new force with forces resulting from internal strains.

This is the basis of the simulation. It is possible to simulate calibration runs utilizing head form configurations without helmets and then simulate test runs with the added helmets and mass in the system.

B. The Configuration

A simple, pseudo-spherical head and helmet were generated to provide for the needs explained in earlier parts of the report. The computer generation program allows regeneration of the configuration with different numbers of elements occupying approximately the same volume in the system. A "packing factor" can be added to the program to adjust each structural region such as the helmet shell to a constant mass as average element size is varied.

The method adopted is to begin with a basic block of cubes and to project the nodal points, into a spherical form. The nodal points on the surface of the basic block are projected radially onto the surface of a

sphere of predetermined radius. The interior nodal points in the basic block are also projected radially but in proportion to their radial distance to the basic block surface. This produces a multi-element group with surface points conforming to the surface of a sphere. Full surrounding shells of elements can be added; and above these, partial shells can be added. These are used to represent the skull and the various significant layers of the helmet and helmet liner.

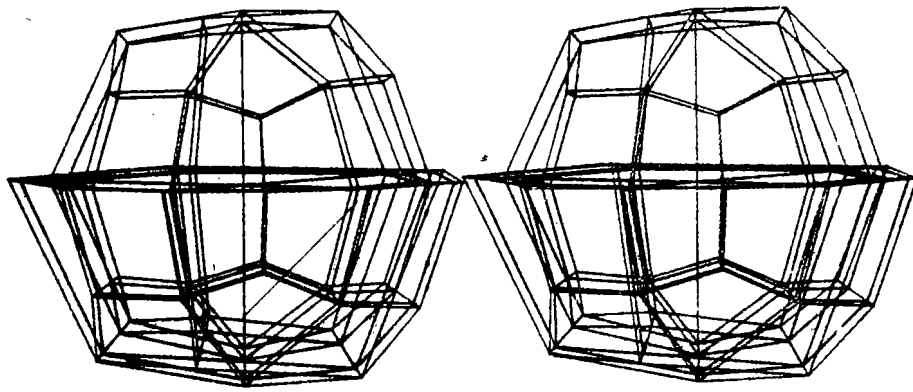
The nodal points of these outer layers are generated to register properly with the surface nodal points from the original projection of the basic block. Thus, there is the desired correspondence throughout the system. Figure 22 shows the configurations for the systems described in Table 6.

Other forms may be adopted in place of the spherical projection surface. Also, other projection schemes may be used to reduce the variation in element volume within the various layers.

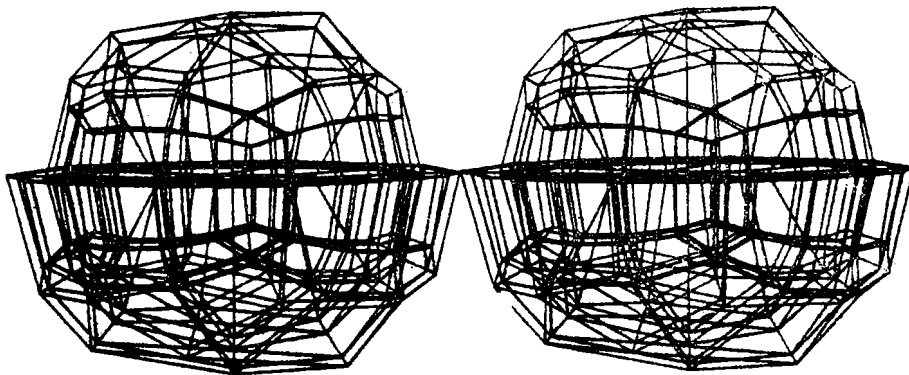
Only the simplest configuration, based on the 3 x 3 x 3 basic block configuration was used in the dynamic analyses.

C. Inertial Properties

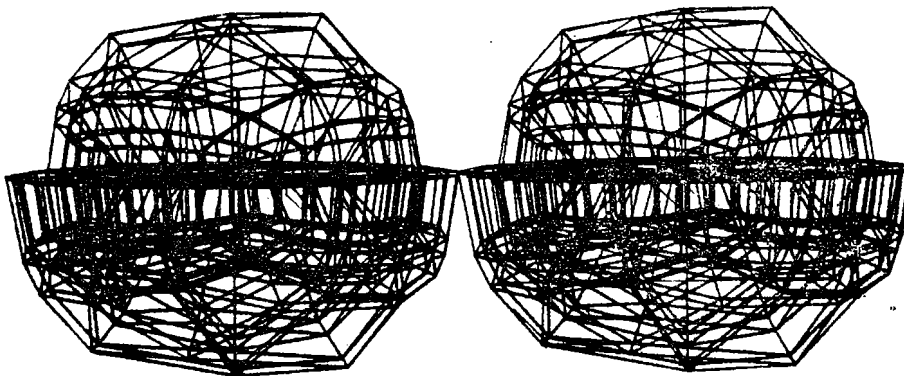
The inertial moments were computed for the head, inner liner, and helmet shell separately and in combination to illustrate the effect of the helmet as an additional load. The results are tabulated in Table 7. The form of the system is shown in Figure 22a. The weight increase is 30.12%, the inertial moment increase is 52.17% about either horizontal axis and 56.46% greater around the vertical axis through the center of gravity. The center of gravity is raised 1.052 cm (lowered 1.052 cm relative to the orientation in the drop test).



a. $3 \times 3 \times 3$



b. $5 \times 5 \times 3$



c. $7 \times 7 \times 3$

Figure 22. Three pseudo-spherical, computer generated head form-helmet models with different meshes for the dynamic simulation.

TABLE 6
PARAMETERS OF THE PSEUDO-SPHERICAL MODELS

a. Common Parameters			
Region	Radius or Thickness (cm)	Youngs Modulus (MPa)	Density (g cm ⁻³)
Aluminum		6.894×10^4	
Brain	8.26	6.894×10	2.1
Skull	0.6	1.6×10^5	3.04
Inner Liner	1.0	6.894×10^{-1}	1.23
Helmet Shell	0.35	6.894×10^4	6.0

b. Structural Units			
Item	Configuration		
	3 x 3 x 3	5 x 5 x 3	7 x 7 x 3
Nodal Points	87	223	415
Elements			
Total	56	160	312
Brain	8	32	72
Skull	24	64	120
Liner	12	32	60
Shell	12	32	60

TABLE 6
PARAMETERS OF THE PSEUDO-SPHERICAL MODELS

c. Computed Volume and Mass			
Item	3 x 3 x 3	Configuration 5 x 5 x 3	7 x 7 x 3
Total Volume, cm ³	2824.8	3193.1	3260.2
Total Mass, kg	6.62	7.49	7.65
Brain, kg	3.80	-	-
Skull, kg	1.29	-	-
Liner, kg	.52	-	-
Shell, kg	1.02	-	-

TABLE 7
INERTIAL PROPERTIES OF THE DYNAMIC MODEL

Region	Coordinates (cm)			Mass (kg)	Inertial Moments (kg cm ²)		
	x	y	z		I _{xc}	I _{yc}	I _{zc}
Head	0	0	0	5.08	170.5	170.5	170.5
Inner Liner	0	0	4.336	0.52	16.1	16.1	25.9
Shell	0	0	4.648	1.01	48.5	48.5	70.4
Helmet	0	0	4.543	1.53	64.7	64.7	96.3
Total	0	0	1.052	6.61	259.5	259.5	266.8

D. Boundary Conditions and Inertial Loading

1. Loading Points

Contact is made with five points on the center of the outside surface of the helmet. These are the lowest points in the configuration as oriented in this simulation. These five points are restricted from motion in the z-direction, of which the center point is totally restricted from motion, and another is sufficiently restricted to prevent any free rotation of the system. All other nodal points are completely free to be displaced due to the action of the deceleration field.

2. Ground Acceleration

In this orientation the helmet is positioned below the head form and together they are dropped onto an arresting surface. The acceleration field acts vertically downwards in the negative z-direction.

A simple triangular acceleration profile was adopted because it is reported to represent the actual acceleration history in these tests. This profile is shown in Figure 23. It is initiated and terminated within a period of 12 milliseconds, reaching its maximum of 400 g at 9 milliseconds after initiation. This can be very easily changed to a trapezoidal or more complicated form by specifying an appropriate time function. Up to 40 points may be used in the specification of the time function. Only 5 are used in the computations reported here.

When the deceleration field is applied the equations of motion become

$$[M]\{\ddot{d}\} + [K]\{\ddot{d}\} + [S]\{d\} = [M]\{-\ddot{d}_{IB}\} \quad [16]$$

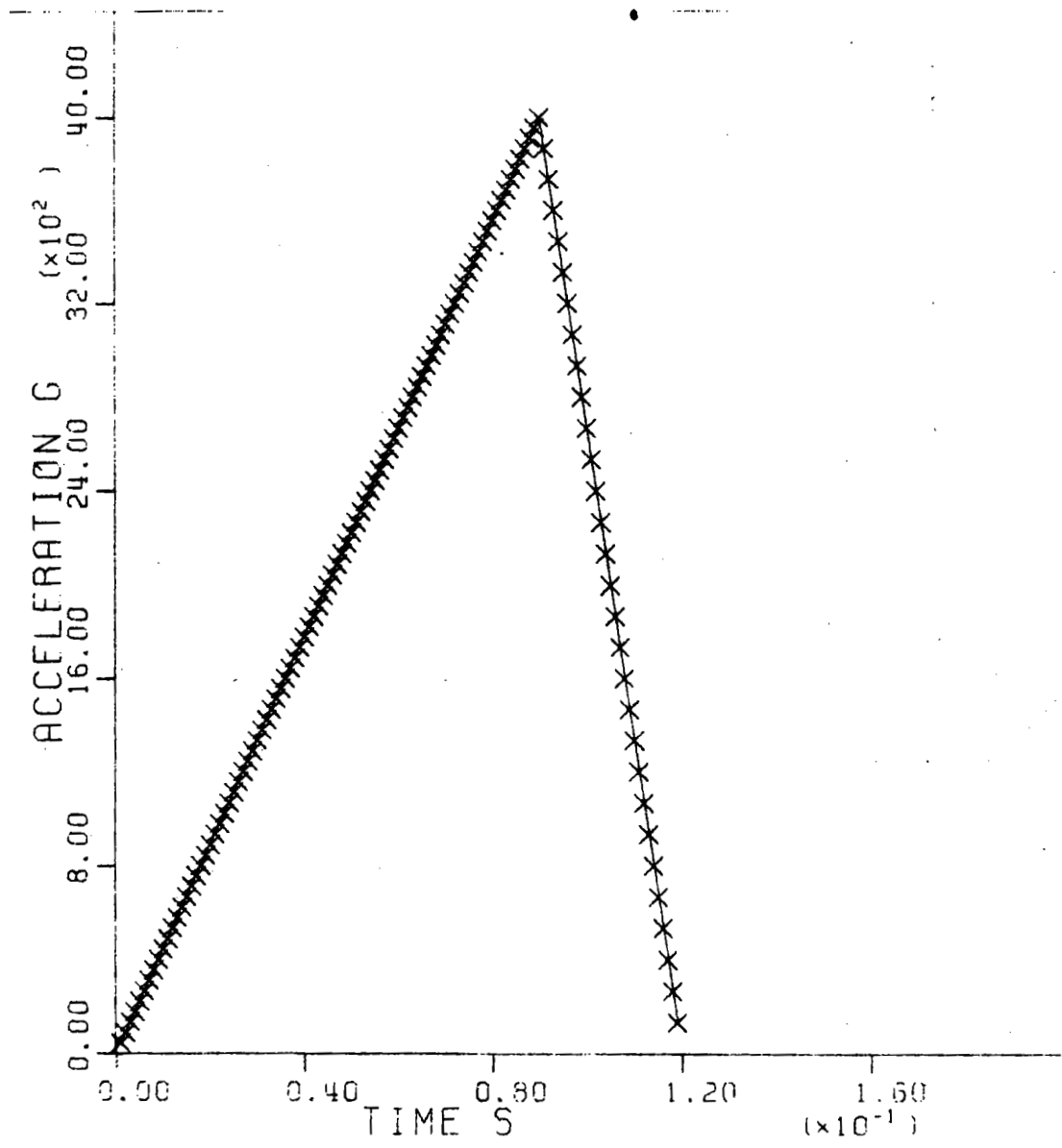


Figure 23. The leading portion of the applied deceleration field profile. The following portion is held at zero.

which is equivalent to Equation [9]. The applied force term of Equation [9] is replaced by the force field due to the deceleration field, $\{-\ddot{d}_{IB}\}$. This field produces inertial body forces in each element. $[M]$ is the matrix of element masses as defined in Equation [9]. Each element generates a force acting on its nodal points due to this field. Each element force depends upon its mass and upon the instantaneous value of the deceleration field which is determined by interpolation from the time function described above.

3. Displacement Time Trace

Equation [16] is solved repeatedly at incremental time steps as specified. The Stiffness, Damping, and Mass matrices are first formulated for the system from nodal point coordinate data, connection array data, and materials property data. The boundary conditions are applied to isolate the degrees of freedom. The matrices in Equation [16] are inverted, (see Equation [8]) and eigenvalues are found to represent the important deformation modes (direct integration can also be performed to bypass this step). Actually all of these steps through the evaluation of the eigenfunctions and the natural frequencies in the system can be performed for a given configuration and the results stored for repeated determinations of displacement and stress time histories.

The following are performed for each time step without repeating the preceding: The body forces are evaluated in each element and partitioned to each nodal point. Any displacements from a prior step are included in the formulation for this step. The displacements are calculated and listed as well as other information called for. The result is a displacement history which is shown in Figure 24 for a basic configuration.

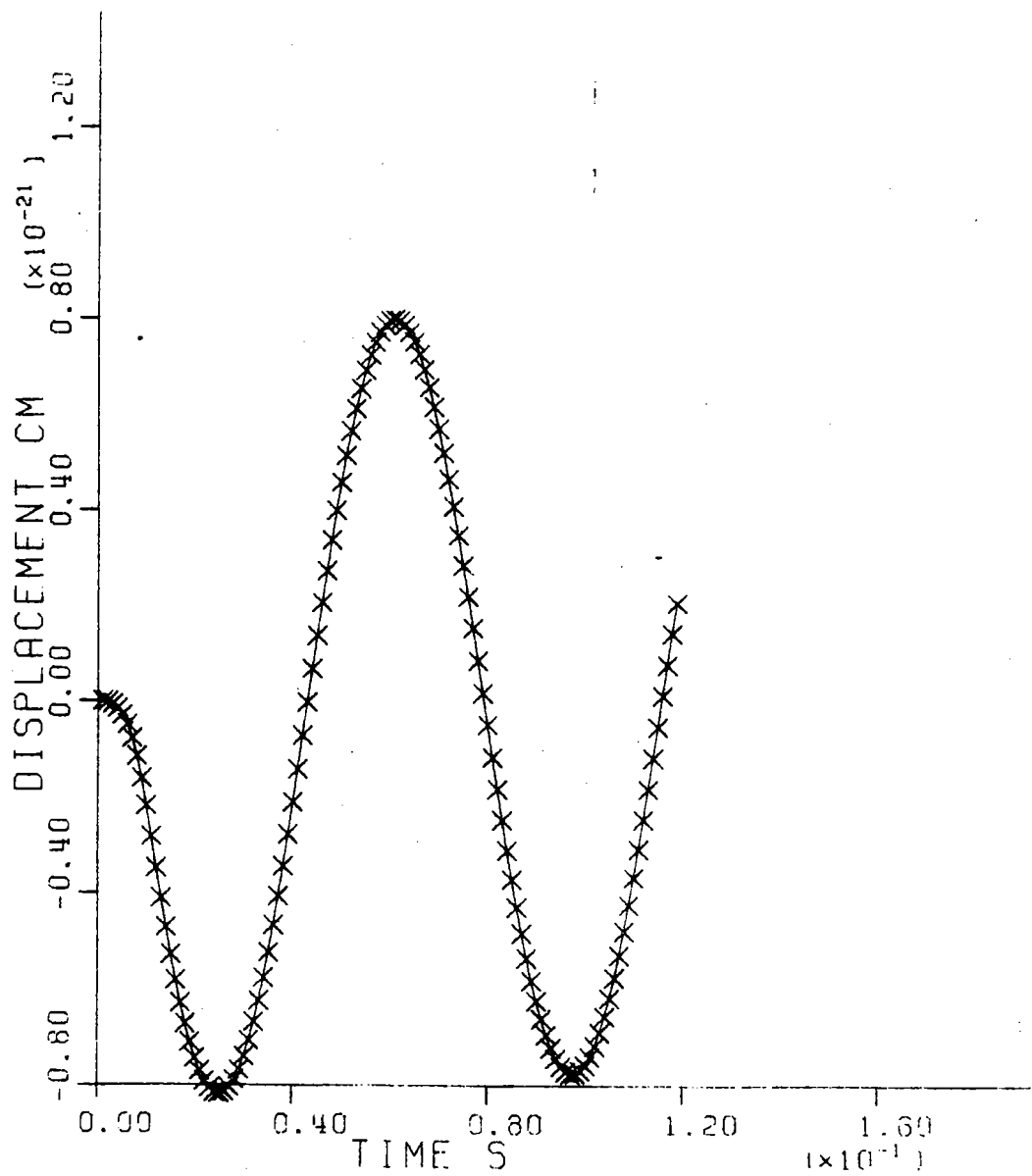


Figure 24. The center-of-gravity displacement for the aluminum head-form with most compliant inner liner (0.6894 MPa)

Figures 24-26 show the time variation of displacement, nodal point velocity, and acceleration of the central nodal point, nodal point 14, in the 3 x 3 x 3 configuration. See Table 5 and APPENDIX B. 120 time steps of 0.0001 second each were used over the total time period.

Figure 27 represents the same structural configuration and test conditions, but with an extended time trace. The period of the analysis is 120 milliseconds, ten times the length of the period of action of the ground motion. The system is seen to go into oscillation, which decays. This is characteristic of all dynamic analyses performed. It will be possible, using the same structural analysis program, but with modified input data, to perform the dynamic analysis with critical damping to better simulate the damping in the real systems.

Therefore each time trace exhibits two parts, the first is when the system is directly driven by the ground acceleration, and the second when it is oscillating. Both the magnitude and frequency of the oscillation are dependent upon the composition and properties of the structural system.

4. Rotational Acceleration

The rotational acceleration of the brain can be represented by the rotational acceleration of a line segment in the brain. The choice of segment may be significant, but there is probably a strong correlation between the rotational accelerations of most line segments that might be chosen. Quite arbitrarily, the segment connecting nodal points 14 (at the centroid of the head) and 15 (immediately adjacent at a physical distance of 8.26 cm along the x-axis) was selected in the spheroidal

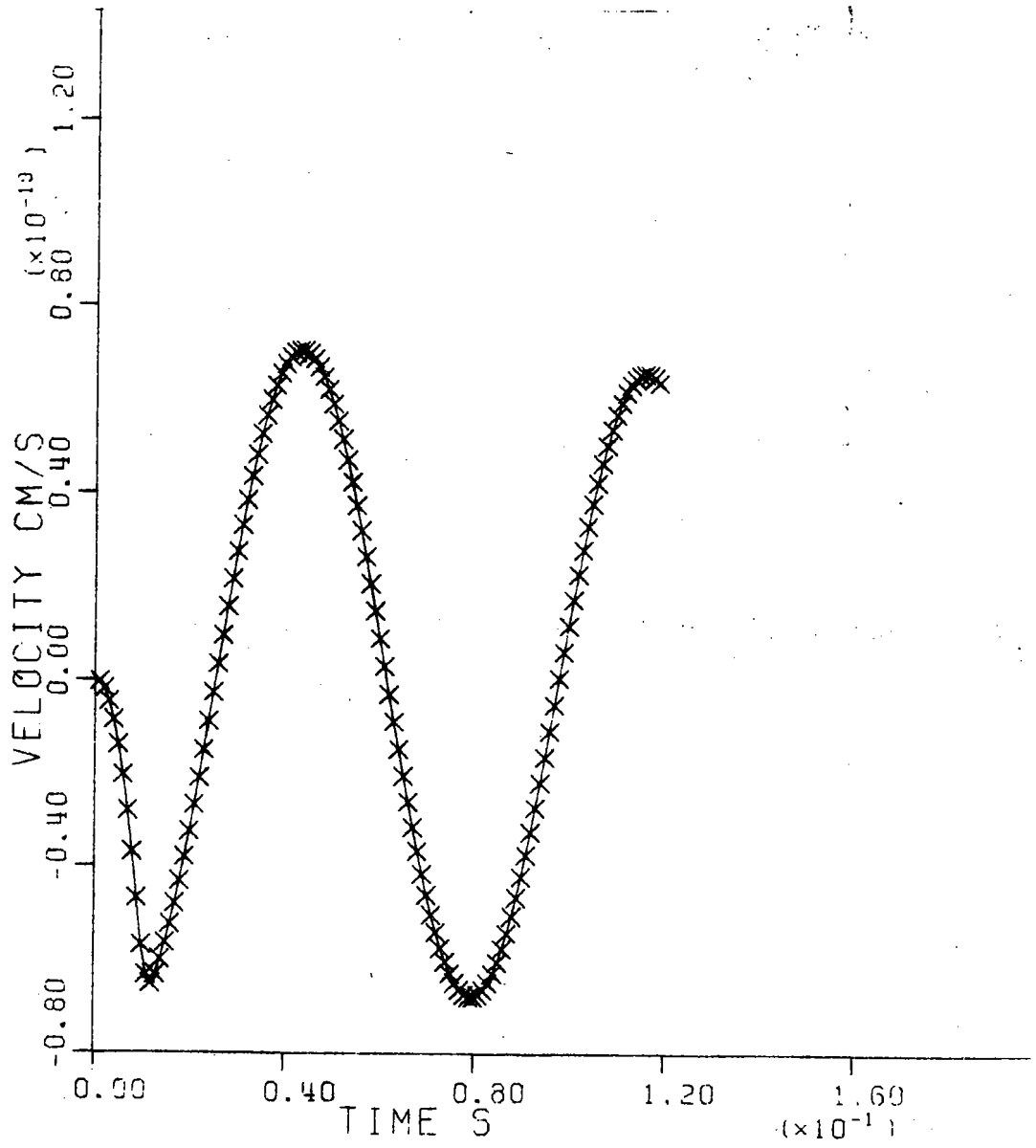


Figure 25. The velocity time trace of the headform center-of-gravity, derived from the data of Figure 24.

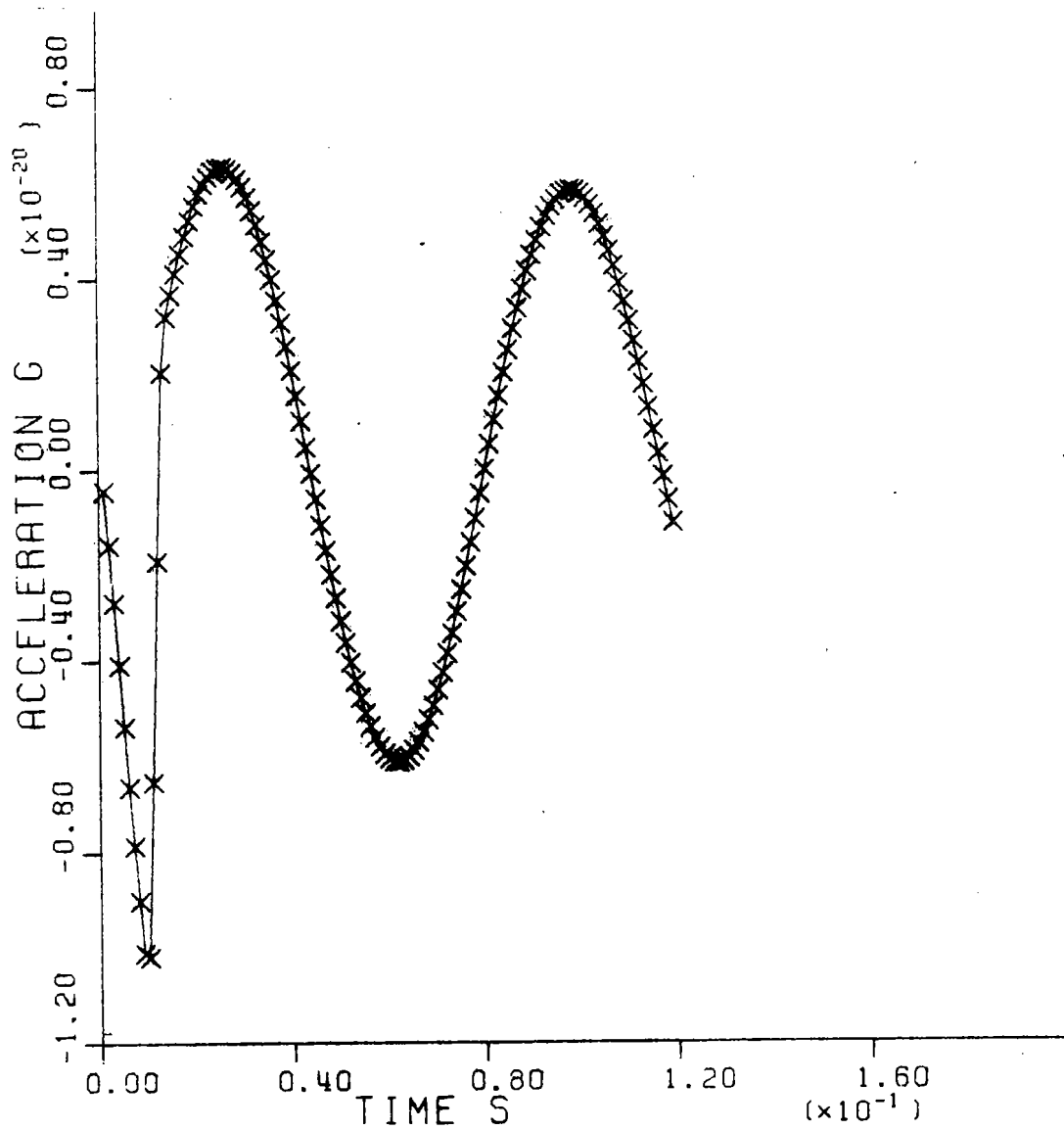


Figure 26. The deceleration time trace of the headform center-of-gravity derived from the data of Figures 24 and 25.

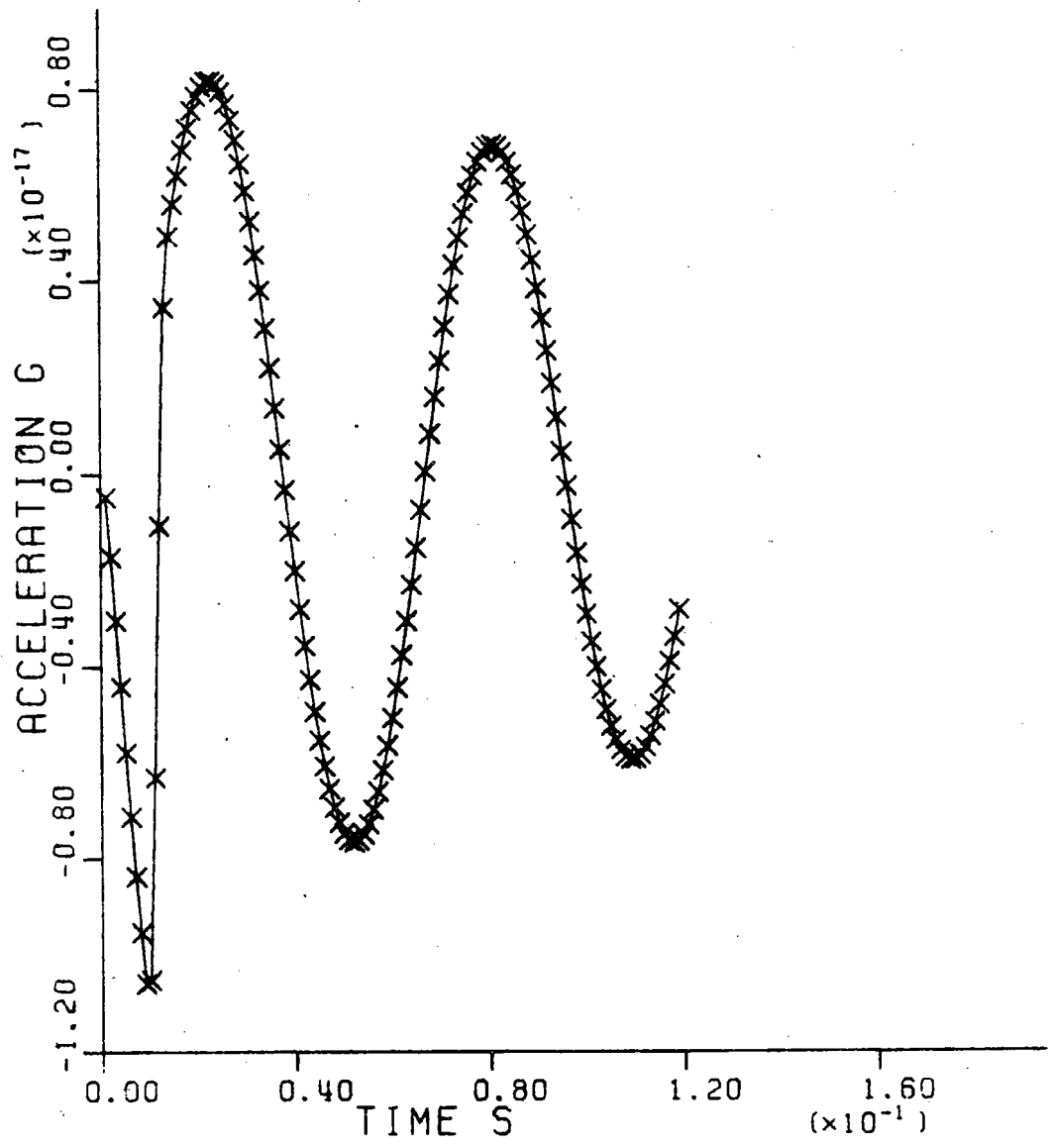


Figure 27. Linear acceleration time trace for the center-of-gravity, which is in the brain of the humanoid head form.

model of the dynamic analysis. Properties of the head were assigned an inner liner modulus of 6.89×10^3 MPa. The angle between the line segment direction and the original direction are computed for each time step from the nodal point displacement time history. Velocity and acceleration histories are obtained by differences.

The results of the rotational acceleration analysis are shown in Figure 28. This too is a decaying oscillation curve which is very similar in form to the linear acceleration time trace. The results show that information is available from the computer simulation and that this type of response should be further examined.

E. Effect of Inner Liner Modulus Variation

1. Aluminum Head Form

The effect of the inner liner modulus on the dynamic results was studied over the same range of modulus variation as with the static analysis of the body-head-helmet system. The same ground motion was applied in each dynamic run. The simplest configuration, based upon a $3 \times 3 \times 3$ basic block, described in Table 5 and shown in Figure 22a, was used. The assigned properties and resulting masses are tabulated in Table 6. Both the brain and skull sections are assigned the modulus of aluminum, but retain the densities of the brain and skull as listed in Table 6.

The results, which follow motion at the center of gravity of the head, are of the same form as the curves shown in Figures 24-28. Each contains two parts, the first shows the effect of the action of ground motion and the final is decaying oscillations. The results are summarized

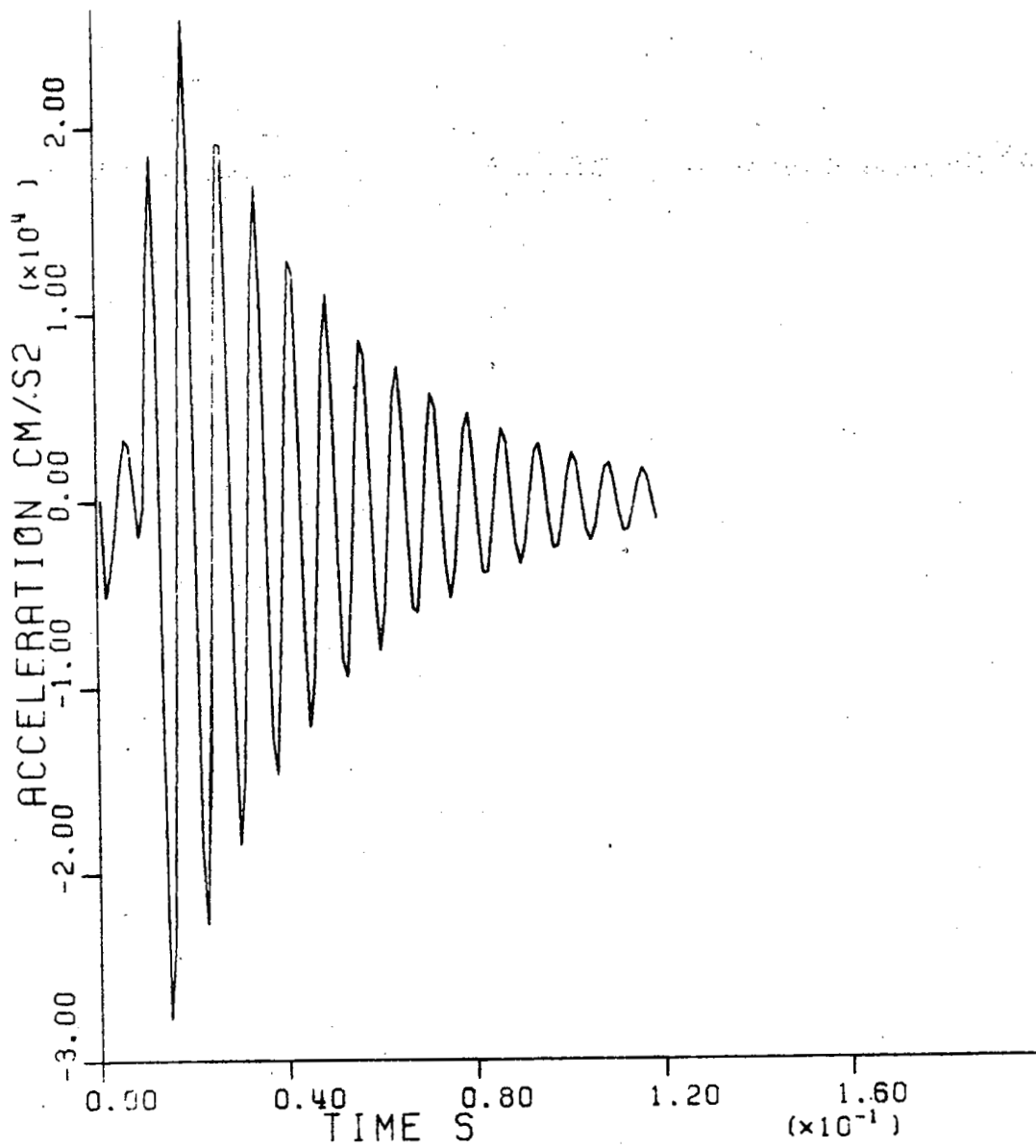


Figure 28. Angular acceleration time trace in the brain of the humanoid head form.

in Table 8, which lists the maximum acceleration listed and the lowest natural frequency on the system. Low modulus inner liner materials are effective in head protection.

2. Humanoid Head Form

An equivalent series of runs was performed with properties of the brain and skull assigned to the corresponding regions in the model. All dimensions and densities were as listed. No properties of aluminum were used. The results are of the same form as those of the aluminum head form but the magnitudes are different. The results are summarized in Table 9. In both series it is obvious that the compliant inner liner absorbs most of the energy in the system. This is apparently exaggerated in the case of the aluminum head form.

3. Severity Index

The dynamic results of the tests with the humanoid head form are used in a demonstration of the computation of the severity index (5). Each acceleration profile was scanned once to compute an average value for the magnitude of the acceleration at the center of gravity of the head. Then a second review of the acceleration data was made to determine the total time over which the head was subjected to this on a higher level of acceleration. The severity index was calculated using Equation [17].

$$SI = (\text{average Acceleration})^{2.5} (\text{exposure time}) \quad [17]$$

Where the average acceleration is in multiples of gravitational acceleration and time is in seconds. Table 10 lists the results of Severity Index for the range of inner liner modulus used.

TABLE 8
 THE EFFECT OF INNER LINER MODULUS ON MAXIMUM ACCELERATION
 AT THE HEAD FORM CENTROID AND NATURAL OSCILLATION
 IN ALL ALUMINUM HEAD FORM

Inner Liner Modulus (MPa)	Maximum Acceleration (cm s ⁻²)	Period Of Oscillation (s)
0.6894	0.621×10^{-17}	0.726×10^{-1}
0.3447×10	0.183×10^{-17}	0.331×10^{-1}
0.6894×10	0.470×10^{-14}	0.240×10^{-1}
0.3447×10^2	0.380×10^{-9}	0.131×10^{-1}
0.6894×10^2	0.586×10^{-9}	0.113×10^{-1}
0.6894×10^3	0.314×10^{-12}	0.846×10^{-2}
0.6894×10^4	0.306×10^{-9}	0.615×10^{-2}

TABLE 9
 THE EFFECT OF INNER LINER MODULUS ON MAXIMUM ACCELERATION
 AT THE HEAD FORM CENTROID AND NATURAL OSCILLATION
 IN THE HUMANOID HEAD FORM

Inner Liner Modulus (MPa)	Maximum Acceleration (cm s ⁻²)	Period Of Oscillation (S)
0.6894	0.801 x 10 ⁻¹⁴	0.726 x 10 ⁻¹
0.347 x 10	0.128 x 10 ⁻¹⁴	0.331 x 10 ⁻¹
0.6894 x 10	0.111 x 10 ⁻¹²	0.240 x 10 ⁻¹
0.3447 x 10 ²	0.383 x 10 ⁻³	0.132 x 10 ⁻¹
0.6894 x 10 ²	0.426 x 10 ⁻³	0.114 x 10 ⁻¹
0.6894 x 10 ³	0.247 x 10 ⁶	0.864 x 10 ⁻²
0.6894 x 10 ⁴	0.230 x 10 ⁶	0.691 x 10 ⁻²

TABLE 10
 THE EFFECT OF INNER LINER MODULUS ON
 SEVERITY INDEX FOR THE HUMANOID HEAD FORM

Inner Liner Modulus (MPa)	SI (g ^{2.5} s)
0.6894	0.355 x 10 ⁻⁴⁴
0.3447 x 10	0.227 x 10 ⁻⁴⁶
0.6894 x 10	0.217 x 10 ⁻⁴¹
0.3447 x 10 ²	0.659 x 10 ⁻¹⁸
0.6894 x 10 ²	0.297 x 10 ⁻¹⁸
0.3447 x 10 ³	0.875 x 10 ³
0.6894 x 10 ⁴	0.714 x 10 ³

V. SUMMARY AND RECOMMENDATIONS FOR FURTHER WORK

The finite element method of analysis is applicable to the simulation of the body-head-helmet system and helmet design. Three dimensional simulation, although relatively demanding of computer facilities, is possible and advantageous especially in the dynamic mode. Analyses were demonstrated on two types of model configurations, fixed and parametric. The computer generated type of configuration is more desirable because it allows parametric representation, automatic variation of mesh size without change in mass, and dependable handling of the voluminous quantity of data involved. Parameters can be provided to specify shape, mass distribution, inertial moment distribution, and materials and systems properties. The results of a finite element analysis yield displacement and stress profiles for a single equilibrium configuration, displacement, velocity, acceleration, and stress histories which represent the time variation of these parameters at any chosen nodal point or element in the system. This is a powerful simulation tool because it can be made to exactly conform to specific input conditions.

A. Inertial Properties Analysis

Size, shape and inertial properties were set and analyzed for both the fixed and parametric models. Section sizes and masses were adjusted to conform to standard (1,4) values. Centers of gravity and inertial moments were computed and compared, where possible, to measured values. Cadaver slices (11) were found to contain considerably lower masses than corresponding fixed model sections. Moments of inertia, adjusted for

this mass difference, compared well about the y-axis, which is directed forward, horizontally. The other two mass adjusted moments are considerably higher than for the model, indicating a difference in mass distribution between the two sections. This is an expected limitation.

B. Structural Analysis

Two types of structural analysis were demonstrated. In one a fixed body-head-helmet configuration was studied under the action of static forces applied to the helmet. The effect of variations of the inner liner modulus over four orders of magnitude were evaluated on displacements in the system and on the maximum normal stresses and maximum shear stresses in elements in the helmet, head, and brain. The results showed that maximum values in each of these parameters are produced when the modulus of elasticity of the inner liner is in the range of 5 to 100 MPa. Above this inner liner stiffness both displacement and shear stress become excessive.

Dynamic analyses were demonstrated on a computer generated configuration based on a spheroidal head shape. This was performed with two models, one representing a human head and the other an aluminum head form, and also for a variation of inner liner modulus. The principal results examined are displacement, velocity, and acceleration in the brain. Stresses are available, although stress histories are not presented in this report. The protection afforded through the inner liner was clearly demonstrated and shown to be limited in approximately the same range of modulus value as for the static determination. Both modes of analysis provide information, but the latter is favored because it more nearly simulates the drop test and other dynamic situations.

The dynamic analyses were performed using the response spectrum mode but future work will probably be performed using the direct integration method which allows control of damping which is more appropriate to the mechanics of the human body.

Variations of these analyses are possible with very little input to the program as presently formulated. A different structural analysis program is available to provide a simulation that includes materials with non-linear behavior.

C. Injury Parameters

A number of parameters of proven or promising merit for the evaluation of human tolerance or severity of impact were evaluated from either the static or dynamic results. The Gadd severity index (5) was computed for the dynamic series, modeled with the head parameters. The results show a similar trend to those of the acceleration magnitude results. Stiff inner liners developed SI values of over 700, which is near critical. The computation of brain angular acceleration was performed for one of the configurations (the stiffest inner liner) of the series. Skull deflection was computed and displayed from the results of the static analysis. The form of the results compared to those published elsewhere on the basis of two (9) and three dimensional (3) finite element analysis.

D. Recommendations for Further Research

The following are recommendations for specific steps to be taken in applying finite element simulation to helmet design:

1. Develop a head form simulation in the dynamic mode with proper damping factor.

2. Add nonlinear and anisotropic material behavior to portions of the system as appropriate. This may apply to both the inner liner and the head form material.
3. Standardize and refine the form of the deceleration field. Develop a procedure to simulate the calibration drop and its results.
4. Develop the computer generated head form simulation by improving the configuration. Possibly use new structure generation algorithms to control size variation of regional elements and to either remove or subdivide (add) elements in the system as appropriate. The parameter or index to govern such operations will be the variation of computed stress between neighboring elements. Perform steps aimed at simplification of the overall configuration prior to production runs or extended study. Compare the results of the simulation with closely related experimental determinations.
5. Develop scanning procedures to establish specific information. Select nodal point displacement components and element normal and shear stress components based on the results of scanning investigations. This may involve subjecting the same configuration to different modes of analysis.
6. Investigate the eccentric system. The system may be eccentric with respect to basic configuration, orientation

relative to the loading system and with respect to the direction in which reactions are followed.

The above can be applied initially to a simple helmet configuration to establish system performance relative to a known experimental system. The effect of variations on the system configuration in terms of materials properties, section dimensions, or the addition of peripheral masses to represent additional equipment such as face shields, gas masks, optical equipment, or audio-communications equipment can then be evaluated. A large proportion of helmet design should be subject to study in this way with relatively little cost compared to that required for prototype fabrication, testing and analysis. Experimental testing is required to establish reference points for comparison to assure the validity of the simulation; but these, too, can be selected on the basis of the results of the simulation.

Experience with this simulation, with respect to the nature of the information available, the amount of computer capacity required and comparisons with published data supports and reinforces the need for the ability to include the "entire" system in the simulation. A general body model, with proper shape, inertial properties and mechanical characteristics can serve as a universal reference for sectioning or full system simulation. This would be available to all investigators for comparison and exchange of information. Finite element techniques can be used to select and simplify such a standard for various specific objectives such as to accommodate simulations on computer systems with different capacities or modes of operation. A

standard mannikin can be "fitted" with any type of helmet, other protective gear, or other equipment and programmed through a sequence of events.

The major future thrust in this line of research will be concerned with efficiency in operation as much as with accuracy in the representation.

VI. CONCLUSIONS

Three-dimensional finite element methods of analysis can be used to evaluate a number of helmet design parameters. Inertial properties of transverse slices of a model of the human thorax were compared with experimental measurements reported by Liu and Wickstrom (11). The mass moments of inertia agreed well about those axes where the distribution of mass in the model agreed with that in the cadavers.

Static, structural analysis was performed on a composite three-dimensional model. This model included the thorax, neck, head and a simple crash helmet. This overall configuration allows the simulation of portions of the body that contribute to the circumstances of numerous crashes. The helmet in this model consisted of a stiff outer shell and compliant energy absorbing liner. Detailed deflections and stress distributions were obtained for this system as a function of inner liner properties. The inner liner modulus was allowed to vary systematically from 10^2 to 10^6 psi (.6894 to $.6894 \times 10^4$ MPa) the results showed that head protection was lost with stiff inner liners.

Static analysis provides useful information where the details of the system and loads are well understood. It was concluded, however, that dynamic structural analysis would furnish more useful information. A simplified, computer generated model was established to simulate the drop test. The model is pseudo-spherical in form, with portions representing various materials. The loading was applied as a general deceleration field. A number of parameters such as head form center-of-gravity,

deceleration profile and Gadd severity index were evaluated as a function of inner liner modulus. The form of these results is in agreement with experimental results reported by Ewing and Thomas (4) and other investigators. It is concluded that dynamic simulation is useful in the design of crash helmets.

BIBLIOGRAPHY

1. Automotive Safety Committee, "Anthropomorphic Test Device for Use in Dynamic Testing of Motor Vehicles," SAE Recommended Practice, SAE J963, (June, 1968).
2. Bathe, Klaus-Jürgen, Edward L. Wilson and Fred E. Peterson, "SAP IV, A Structural Analysis Program for Static and Dynamic Response of Linear Systems," Report No. EERC 73-11, (June, 1973).
3. Chan, Han Sun, "Mathematical Model for Closed Head Impact," Proc. Eighteenth Stapp Car Crash Conf., SAE, (December, 1974), 557.
4. Ewing, Channing L., and Daniel J. Thomas, "Human Head and Neck Response to Impact Acceleration," NAMRL Monograph 21, USAARL 73-1, (August, 1972).
5. Gadd, C. W., "Use of a Weighted-Impulse Criterion for Estimating Injury Hazard," Proc. Tenth Stapp Car Crash Conference, SAE, (November, 1966).
6. Goss, Charles M., Gray's Anatomy, 29th Ed., Lea & Febiger, (1974).
7. Gurdjian, E. S., H. R. Lissner, and L. M. Patrick, "Protection of the Head and Neck in Sports," J.A.M.A., 182 #5, (1962), 509-512.
8. Haley, J. L., Jr., J. W. Turnbow, S. Macri, and G. J. Walhout, "Helmet Design Criteria for Improved Crash Survival," USAAVLABS Technical Report 65-44, (January, 1966).
9. Hardy, Claude H. and Pedro V. Marcal, "Elastic Analysis of a Skull," Task Order NR 064-512, TR-8, Brown University, (November, 1971).
10. Holbourne, A. H. S., "Mechanics of Head Injuries," Lancet, 245, (1943), 438-441.
11. Liu, Y. King, and Jack K. Wickstrom, "Estimation of the Inertial Property Distribution of the Human Torso From Segmented Cadaverick Data," Perspectives in Biomedical Engineering, MacMillan, (1973), 203-213.
12. Lombard, Charles F., W. Ames Smith, Herman P. Roth and Sheldon Rosenfeld, "Voluntary Tolerance of the Human to Impact Accelerations of the Head," J. Aviation Med., 22, (1951) 109-116.